Supplementary Information

High Yield, Low-Waste Synthesis of a Family of Pyridyl and Imidazolyl-Substituted Schiff Base Linker Ligands

Rana Sanii,[†] Alankriti Bajpai,[†] Ewa Patyk-Kaźmierczak[†‡] and Michael J. Zaworotko*[†]

[†]Department of Chemical Sciences and Bernal Institute, University of Limerick, Castletroy, Co. Limerick, Ireland.
[‡]Department of Materials Chemistry, Faculty of Chemistry, Adam Mickiewicz University, Umultowska 89b, 61-614, Poznań, Poland.

*e-mail: Michael.Zaworotko@ul.ie

Table of Contents

Chart S1. Library of synthesized Schiff base compounds **1**-**8** with atoms labelled corresponding to the crystal structures. In crystal information files atom labels of molecules of compounds crystallizing with more than one conformer in the asymmetric part of the unit cell include a letter suffixes (A or B). However, only one version of the label was included in the chart for clarity. For molecules laying on the symmetry elements, only atoms belonging to the asymmetric part of the molecule were labelled.

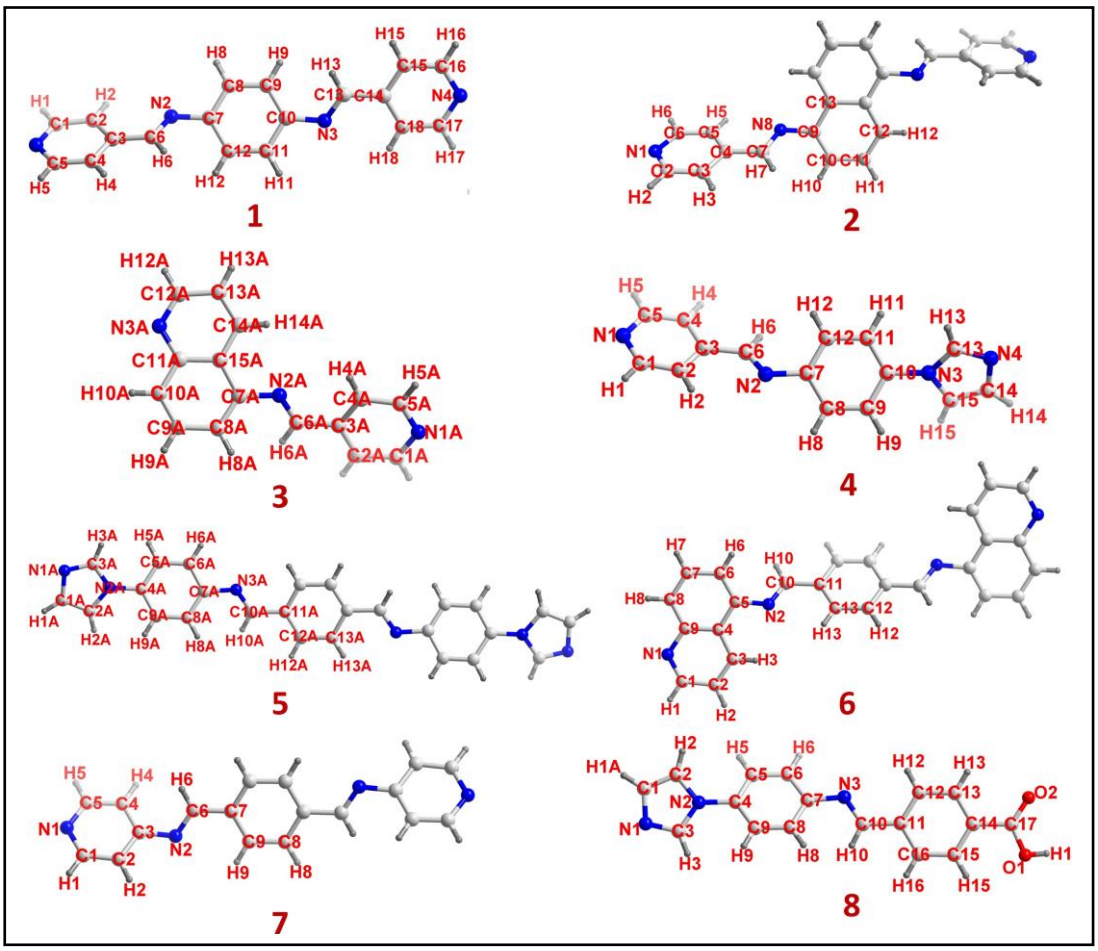

Methods and Materials

General aspects

Reagents and solvents were procured from Sigma Aldrich, Fluorochem or TCI and used as received. S^3 reactions were performed using a Retsch MM400 shaker mill in a 10 mL steel vessel with one 10 mm steel balls at 30 Hz for the specified time. In order to increase friction in conducting milling experiments, particularly compounds **1**-**4** that are prepared from an aldehyde that is a liquid, two 10 mm steel balls were used. ^{1}H and ^{13}C Nuclear Magnetic Resonance (NMR) spectra were recorded on a Jeol EX270 or ECX400. Powder X-ray diffraction (PXRD) data were measured on Empyrean diffractometer (PANalytical, Philips) using Cu$K\alpha$ source. Data were collected from 4 to 40˚ 2θ with a step size of 0.02˚ and a scan rate of 0.1˚ min^{-1}. Thermogravimetric Analyses (TGA) were performed on a TA Instrument Q50 TG from ambient temperature to 500 °C under a 60 mL min^{-1} flow of N_2, at a scan rate of 20 °C min^{-1}. Differential Scanning Calorimetry (DSC) analyses were carried out on a TA

Instrument DSC Q20 from ambient temperature to the melting point of the final product at a scan rate of 20 °C min^{-1}. Fourier Transform Infrared (FTIR) spectra were collected on a Perkin Elmer Spectrum 100 spectrometer with Universal ATR accessory between the range of 4000-650 cm^{-1}.

X-ray crystallography

Crystal structures of all synthesized compounds were determined by single crystal X-ray diffraction (SCXRD). Measurements were performed at 100(2) K (**1**•H_2O, **3**•(x)H_2O, **5**, **6**•1.4H_2O•0.6MeOH, ***7α***, ***7β***, **7•AMP**, **7**•4H_2O and sql-5-Ni-4i), 273(2) K (**4**) or 298(2) K (**2** and **8**) with either Mo*Kα* (*λ* = 0.71073 Å) or Cu*Kα* (*λ* = 1.5418 Å) radiation and Bruker D8 Quest fixed-chi diffractometer equipped with Photon II or Photon 100 detector, and the nitrogen-flow Oxford Cryosystem attachment. Unit-cell determination, data reduction and absorption correction (multi-scan method) were conducted using the Bruker APEX3 suite with implemented SADABS software.[1] OLEX2 software containing ShelX package was used for structure solution and refinement.[2] All structures were solved by intrinsic phasing or direct methods with programs ShelXT-2014 or ShelXS-2008, respectively, and were refined with program ShelXL-2014 using the least-squares method.[3,4,5] All non-hydrogen atoms were refined anisotropically. Hydrogen atoms were located at idealized positions based on the molecular geometry and assigned isotropic thermal parameters depending on the equivalent displacement parameters of their carriers. Detailed crystallographic information for all structures is listed in Tables S3 and S4.

Synthesis of Compounds 1-8

Bis(pyridin-4-ylmethylene)benzene-1,4-diamine (1).

Compound **1** has been previously reported and prepared by refluxing the starting materials in the presence of an acid.[6] In our modified procedure, *p*-phenylenediamine (0.11 g, 1.0 mmol) and 4-pyridinecarboxaldehyde (0.21 g, 2.0 mmol) were ground until a free-flowing yellow powder was obtained. Upon addition of ~100 µL of MeOH the resultant yellow paste was further ground (*ca.* 10 min) until a free-flowing deep yellow powder was obtained as pure product. Compound **1** was also prepared by milling of *p*-phenylenediamine (0.86 g, 8.0 mmol) and 4-pyridinecarboxaldehyde (1.71 g, 16.0 mmol) with the addition of ~100 µL of MeOH for 15 min; yield 98.0%. Alternately, compound **1** was also prepared by dropwise addition of 4-pyridinecarboxaldehyde (0.21 g, 2.0 mmol) to a solution of *p*-phenylenediamine (0.11 g, 1.0 mmol) in 3 mL of MeOH using a microsyringe. The colour of solution changed from light pink to deep orange. The contents were allowed to stir at rt for 15 min. The completion of reaction was monitored by thin layer chromatography (TLC) analysis and the solvent removed *in vacuo* on complete consumption of the starting materials. Pure product was isolated as a yellow solid by recrystallization using MeOH and subsequent heating at 100˚C in 95.4% yield. M.p. 182-186 ˚C; FTIR (ATR) cm^{-1} 1624 ($\nu_{CH=N}$); ^{1}H NMR (270 MHz, $CDCl_3$) δ 7.44 (s, 4H), 7.85 (d, 4H, J = 5.94 Hz), 8.75 (d, 4H, J = 5.94 Hz), 8.74 (s, 2H); ^{13}C NMR (67.5 MHz, $CDCl_3$) δ 122.1, 122.4, 142.4, 149.1, 150.4, 158.9.

N,N'-Bis(4-pyridylmethylene)naphthalene-1,5-diamine (2).

Compound **2** has been previously reported and synthesized by stirring the reactants in an EtOH solution containing formic acid for 4 h.[7] In our modified procedure a new polymorph of compound **2** was isolated. 1,5-Diaminonaphthalene (0.08 g, 0.5 mmol) and 4-pyridinecarboxaldehyde (0.11 g, 1.0 mmol) were ground until a free-flowing yellow powder was obtained. Upon addition of ~100 µL of MeOH the resultant yellow paste was further ground (*ca.* 10 min) until a free-flowing deep yellow powder was obtained as pure product. Compound **2** was also prepared by milling of 1,5-diaminonaphthalene (1.26 g, 8.0 mmol) and 4-pyridinecarboxaldehyde (1.71 g, 16.0 mmol) with the addition of ~100 µL of MeOH for 15 min. Yield 98.6%; Alternately, compound **2** was prepared by dropwise addition of 4-pyridinecarboxaldehyde (0.11 g, 1.0 mmol) to a solution of 1,5-diaminonaphthalene (0.08 g, 0.5 mmol) in 8 mL of MeOH/$CHCl_3$ (1:1 *v/v*) mixture. Upon completion of reaction, as determined by TLC analysis, the solvent was removed *in vacuo* and pure product recrystallized using MeOH/$CHCl_3$ (1:1 *v/v*) as a yellow solid; 97.5% yield; m.p. 252-258 ˚C; FTIR (ATR) cm^{-1} 1620 ($\nu_{CH=N}$); ^{1}H NMR (270 MHz, $CDCl_3$) δ 7.16 (d, 2H, J = 7.18 Hz), 7.53 (t, 2H, J = 7.78 Hz), 7.88 (d, 4H, J = 5.18 Hz), 8.28 (d, 2H, J = 8.67 Hz), 8.58 (s, 2H), 8.81 (d, 4H, J = 5.18 Hz); ^{13}C NMR (67.5 MHz, $CDCl_3$) δ 113.9, 122.1, 122.4, 126.3, 128.8, 142.5, 147.3, 150.5, 159.8.

***N*-(pyridin-4-ylmethylene)quinolin-5-amine (3).**

5-Aminoquinoline (0.14 g, 1.0 mmol) and 4-pyridinecarbxaldehyde (0.10 g, 1.0 mmol) were ground until a free-flowing yellow powder was obtained. Upon addition of ~100 µL of MeOH the resultant yellow paste was further ground (*ca.* 10 min) until a free-flowing deep yellow powder was obtained as pure product. Compound **3** was also prepared by milling of 5-aminoquinoline (1.15 g, 8.0 mmol) and 4-pyridinecarboxaldehyde (0.85 g, 8.0 mmol) with the addition of ~100 µL of MeOH for 15 min; yield 98.5%. Alternately, compound **3** was also prepared by dropwise addition of 4-pyridinecarboxaldehyde (0.10 g, 1.0 mmol) to a solution of 5-aminoquinoline (0.14 g, 1.0 mmol) in 2.5 mL of MeCN. Colour of the solution instantaneously changed from pale yellow to deep yellow. The contents were allowed to stir at rt for 10 min to ensure the completion of reaction after which the contents were concentrated *in vacuo.* Pure product was isolated as a yellow solid upon recrystallization using MeCN as solvent; 97.0% yield. TGA revealed a variable weight loss of 7-9% at ~75 ˚C (Figure S12). The yellow solid was further heated at 75 ˚C for 2 h to isolate anhydrous product. M.p. 91-94 ˚C. FTIR (ATR) cm^{-1} 1602 ($\nu_{CH=N}$); ^{1}H NMR (270 MHz, DMSO-d_6) δ 7.45 (d, 1H, J = 7.76 Hz), 7.58 (dd, 1H, J = 8.53 Hz), 7.80 (t, 1H, J = 7.92 Hz), 7.95 (s, 1H), 7.98-8.01 (m, 2H), 8.73 (d, 1H, J = 7.76 Hz), 8.80-8.84 (m, 3H), 8.97 (d, 1H, J = 4.21 Hz); ^{13}C NMR (67.5 MHZ, DMSO-d_6) δ 113.8, 121.6, 122.5, 123.7, 127.5, 129.7, 132.0, 142.4, 147.4, 148.0, 150.6, 151.1, 160.7.

***N,N*'-4-(1H-imidazol-1-yl)-*N*-(pyridin-4-ylmethylene)aniline (4).**

4-(1H-imidazol-1-yl)aniline (0.16 g, 1.0 mmol) and 4-Pyridinecarboxaldehyde (0.11 g, 1.0 mmol) were ground until a free-flowing powder was obtained. Upon addition of ~100 µL of 2-propanol the resultant paste was further ground (*ca.* 10 min) until a free-flowing light brown powder was obtained as pure product. Compound **4** was also prepared by milling of 4-(1H-imidazol-1-yl)aniline (1.27 g, 8.0 mmol) and 4-pyridinecarboxaldehyde (0.85 g, 8.0 mmol) with the addition of ~100 µL of 2-propanol for 15 min. Alternately, compound **4** was also prepared by dropwise addition of 4-Pyridinecarboxaldehyde (0.11 g, 1.0 mmol) to a saturated solution of 4-(1H-imidazol-1-yl)aniline (0.16 g, 1.0 mmol) in 2.5 mL of DMF/MeOH (1:4 *v/v*) mixture. The colourless solution instantaneously changed to dark brown. The contents were allowed to stir at rt for 20 min and concentrated *in vacuo*. Recrystallization of crude solid using MeOH yielded compound **4** as a pale yellow solid; 97.5% yield; m.p. 130-134 ˚C; FTIR (ATR) cm^{-1} 1629 ($\nu_{CH=N}$); ^{1}H NMR (270 MHz, DMSO-d_6) δ 7.13 (s, 1H), 7.50 (d, 2H, J = 8.90 Hz), 7.75 (d, 2H, J = 8.90 Hz), 7.80 (s, 1H), 7.86 (d, 2H, J = 6.06 Hz), 8.32 (s, 1H), 8.76 (s, 1H), 8.76 (d, 2H, J = 6.06 Hz). ^{13}C NMR (67.5 MHz, $CDCl_3$) δ 117.9, 121.0, 122.2, 122.7, 129.9, 135.5, 135.6, 142.3, 148.7, 150.4, 159.6.

***N,N*'-(1,4-phenylenebis(methan-1-yl-1-ylidene))bis(4-(1H-imidazol-1-yl)aniline) (5).**

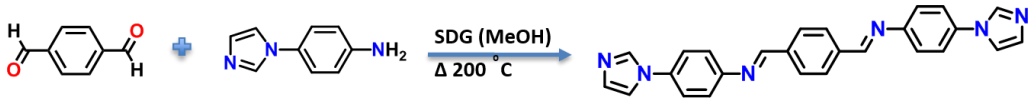

Terephthalaldehyde (0.13 g, 1.0 mmol) and 4-(1H-imidazol-1-yl)aniline (0.31 g, 2.0 mmol) were ground until a free-flowing powder was obtained. Upon addition of ~100 µL of MeOH the resultant paste was further ground (*ca.* 10 min) until a free-flowing deep yellow powder was obtained. TGA revealed a weight loss of 1.6% at 200 ˚C (Figure S20). Hence, this deep yellow solid was heated at 200 ˚C for 3 h to isolate pure product as a dark brown solid. Compound **5** was also prepared by milling of terephthalaldehyde (0.67 g, 5.0 mmol) and 4-(1H-imidazol-1-yl)aniline (1.59 g, 10.0 mmol) with the addition of ~100 µL of MeOH for 5 min. The final product was also obtained by dry milling the starting materials for 20 min. Yield 98.0%; m.p. > 300 ˚C; FTIR (ATR) cm^{-1} 1623 ($\nu_{CH=N}$). ^{1}H NMR (270 MHz, DMSO-d_6) δ 7.12 (s, 2H), 7.49 (d, 4H, J = 8.79 Hz), 7.74 (d, 4H, J = 8.79 Hz), 7.80 (s, 2H), 8.11 (s, 4H), 8.31 (s, 2H), 8.80 (s, 2H); ^{13}C NMR (67.5 MHz, DMSO-d_6) δ 118.0, 121.1, 122.6, 129.1, 129.9, 135.0, 135.4, 138.4, 149.4, 160.3.

***N,N'*-(1,4-phenylenebis(methan-1-yl-1-ylidene))diquinolin-5-amine (6).**

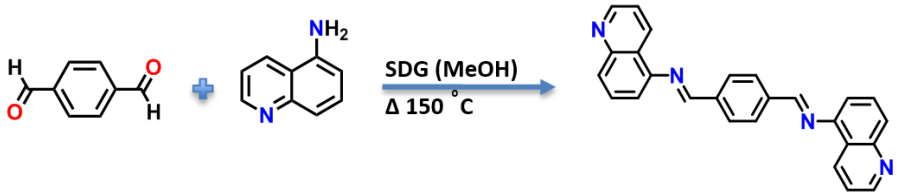

Terephthalaldehyde (0.13 g, 1.0 mmol) and 5-aminoquinoline (0.23 g, 2.0 mmol) were ground into the fine powder. Subsequently, ~100 µL of MeOH was added and further ground until the paste turned into a free-flowing yellow powder (*ca.*10 min). TGA revealed a variable weight loss of 8-15% at 150 ˚C (Figure S24). To isolate the pure anhydrous product, the yellow solid was heated at 150 ˚C for 2 h. Compound 6 was also prepared by milling of terephthalaldehyde (0.67 g, 5.0 mmol) and 5-aminoquinoline (1.44 g, 10.0 mmol) with the addition of ~100 µL of MeOH for 5 min. Deep yellow solid was obtained as pure product; yield 98.5%; m.p. 227-231 ˚C.; FTIR (ATR) cm^{-1} 1616 ($\nu_{CH=N}$); ^{1}H NMR (270 MHz, DMSO-d_6,) δ 7.45 (d, 2H, J = 7.18 Hz), 7.60 (dd, 2H, J = 8.42 Hz, J = 4.20 Hz), 7.81 (t, 2H, J = 7.91 Hz), 7.95 (d, 2H, J = 8.40 Hz), 7.95 (d, 2H, J = 8.40 Hz), 8.27 (s, 4H), 8.67 (d, 2H, J = 9.45 Hz), 8.90 (s, 2H), 8.97 (dd, 2H, J = 4.10 Hz, J = 1.45 Hz); ^{13}C NMR (67.5 MHz, DMSO-d_6) δ 113.5, 121.3, 123.8, 127.0, 129.4, 129.7, 131.8, 138.6, 147.9, 148.0, 151.0, 161.3.

***N,N'*-(1,4-phenylenebis(methan-1-yl-1-ylidene))dipyridine-4-amine (7).**

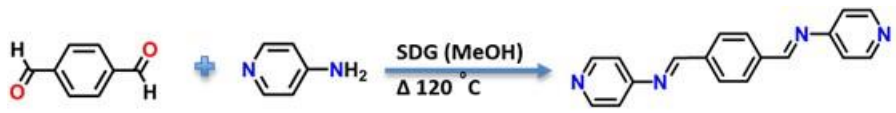

Compound **7** has been previously reported and prepared by refluxing the starting materials in the presence of an acid.[8] In our modified procedure, terephthalaldehyde (0.13 g, 1.0 mmol) and 4-aminopyridine (AMP) (0.19 g, 2.0 mmol) were ground until a free-flowing powder was obtained. Upon addition of ~100 µL MeOH the resultant mixture (paste) was further ground (*ca.* 10 min) until a free-flowing white powder was obtained. PXRD revealed presence of unreacted starting materials. Hence, the powder was heated at 120 ˚C for 1 h for completion of reaction. As a result, yellow needle-shaped crystals were obtained. To isolate pure product, the heated sample was recrystallized from acetone,

acetonitrile and ethanol. Yield 95.2%; m.p. 243-252 ˚C; FTIR (ATR) cm^{-1} 1621 ($\nu_{CH=N}$); ^{1}H NMR (270 MHz, DMSO-d_6) δ 7.24 (d, 4H, J = 5.25 Hz), 8.12 (s, 4H), 8.57 (d, 4H, J = 5.25 Hz), 8.71 (s, 2H); ^{13}C NMR (67.5 MHZ, DMSO-d_6) δ 115.9, 129.6, 138.2, 150.7, 163.4.

4-((4-(1H-imidazol-1-yl)phenylimino)methyl)benzoic acid (8).

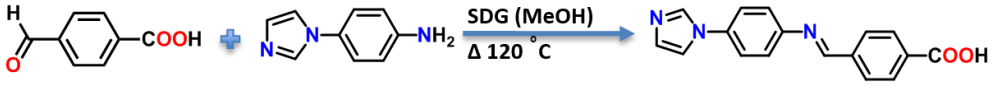

4-Carboxybenzaldehyde (0.15 g, 1.0 mmol) and 4-(1H-imidazol-1-yl)aniline (0.16 g, 1.0 mmol) were ground with ~100 µL of MeOH using an agate mortar and pestle until a pale yellow coloured powder was obtained (*ca.* 10 min). TGA revealed a weight loss of 8.9% at 100 ˚C (Figure S33). Hence, this pale yellow solid was heated at 100 ˚C for 5 h to obtain product as yellow solid. Pure product was isolated by recrystallization from $CHCl_3$/MeOH (1:1 *v/v*) mixture. Compound **8** was also prepared by milling of 4-carboxybenzaldehyde (0.75 g, 5.0 mmol) and 4-(1H-imidazol-1-yl)aniline (0.79 g, 5.0 mmol) with the addition of ~100 µL of MeOH for 5 min. Yield 97.0%; m.p. 286-296 ˚C; FTIR (ATR) cm^{-1} 1627 ($\nu_{CH=N}$). ^{1}H NMR (270 MHz, DMSO-d_6) δ 8.80 (s, 1H), 8.31 (s, 1H), 8.07 (s, 4H), 7.80 (s, 1H), 7.74 (d, 2H, J = 8.65 Hz), 7.48 (d, 2H, J = 8.65 Hz), 7.12 (s, 1H). ^{13}C NMR (67.5 MHZ, DMSO-d_6) δ 114.1, 121.1, 122.6, 128.8, 129.5, 130.0, 133.2, 135.6, 135.8, 139.5, 149.3, 160.3, 166.9.

Synthesis of Compound sql-5-Ni-4i ($C_{52}H_{40}N_{14}NiO_6$).

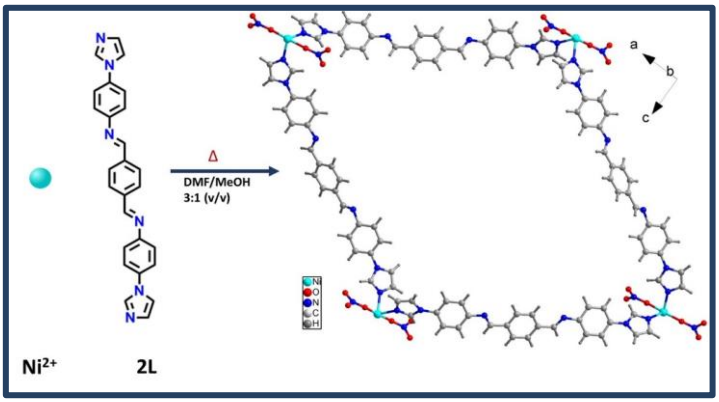

A mixture of $Ni(NO_3)_2{\cdot}6H_2O$ (0.01 g, 0.05 mmol) and N,N'-(1,4-phenylenebis(methan-1-yl-1-ylidene))bis(4-(1H-imidazol-1-yl)aniline (**5**) (0.04 g, 0.1 mmol) dissolved in 4 mL of DMF/MeOH (3:1 v/v). The vial was sealed and heated at 120 ˚C for two days. The reaction system was cooled to room temperature at a rate of 10 ˚C per hour. Yellow uneven single crystals suitable for single-crystal X-ray diffraction were obtained; yield 67%.

Characterization of Compounds 1-8

Bis(pyridin-4-ylmethylene)benzene-1,4-diamine (1).

As revealed by PXRD, SDG of the starting materials using methanol provided the anhydrate (PEXXEW) form of **1**. However, milling the starting materials in presence of methanol resulted in monohydrate (HIRLUQ) form of **1** (Figure S1). TGA profile of the monohydrate form of **1** revealed a weight loss of 5.4% at ~75 ˚C, corresponding to the water molecule present in the crystal structure (Figure S4). The FTIR spectra of compound **1** (purple and green) exhibits shifts in the carbonyl and primary amine region when compared to pure aldehyde (blue) and amine (red) (Figure S5).

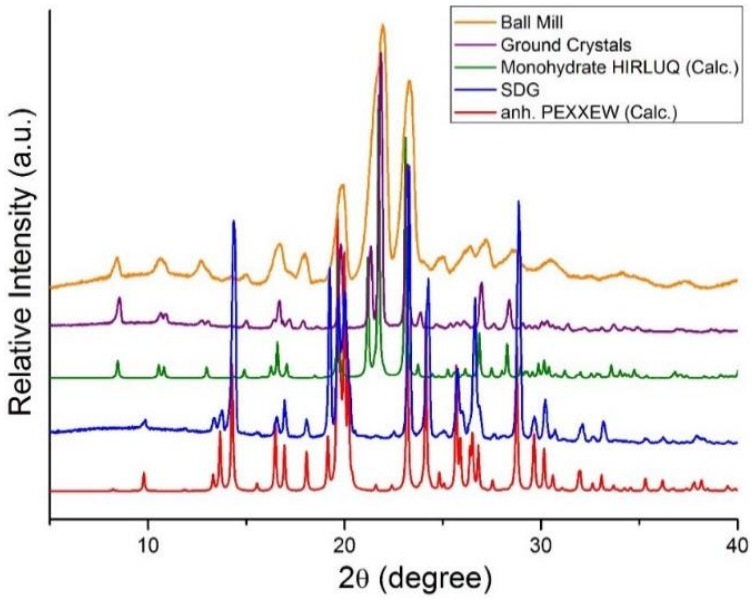

Figure S1. Calculated PXRD of anhydrate form of **1** (red) is consistent with the compound **1** obtained *via* Solvent-Drop Grinding with methanol (blue). Calculated PXRD of monohydrate of **1** (green) is consistent with compound **1** obtained *via* ball-milling with methanol (orange) and ground crystals of compound **1** (purple) obtained after recrystallization of compound **1**.

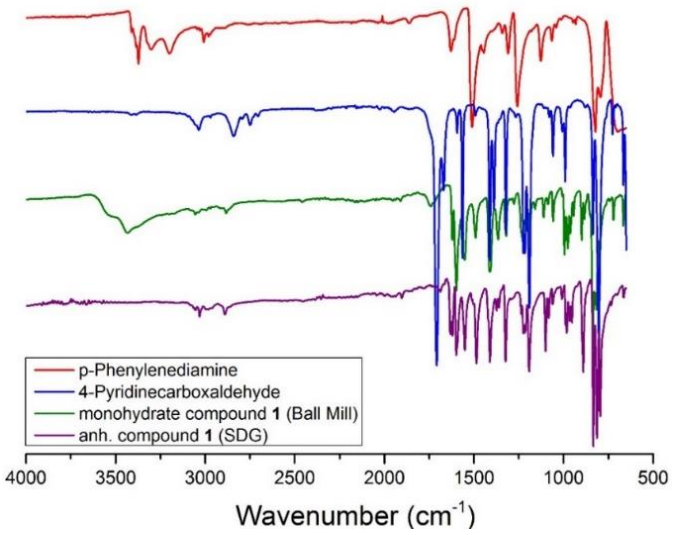

Figure S2. The FTIR spectra of anhydrate form of **1** (purple) obtained *via* solvent-drop grinding of *p*-phenylenediamine (red) and 4-pyridinecarboxaldehyde (blue) with methanol compared with the monohydrate form of **1** (green) obtained *via* ball-milling of the starting materials with methanol.

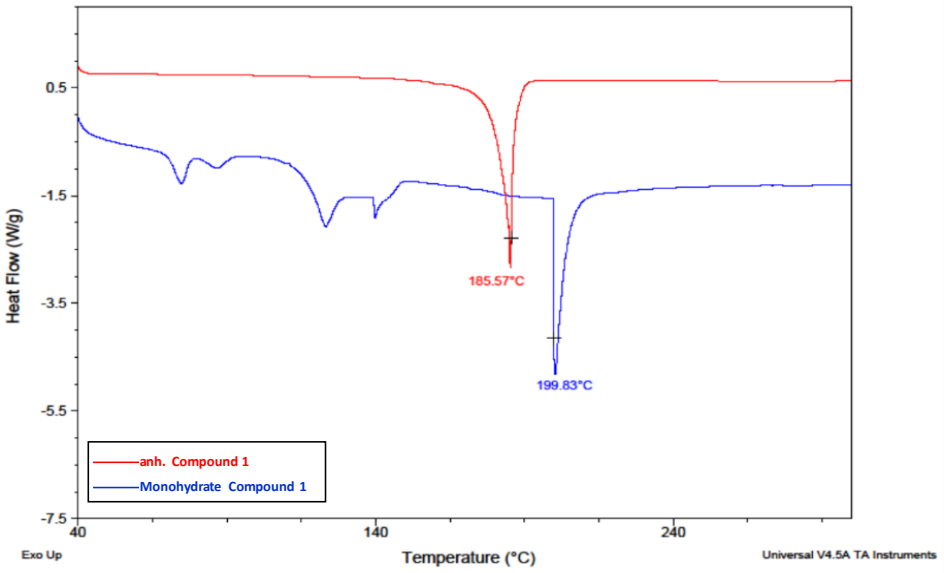

Figure S3. The DSC profiles of anhydrate form of compound **1** obtained *via* SDG (red) and monohydrate form of compound **1** obtained *via* ball-milling (blue).

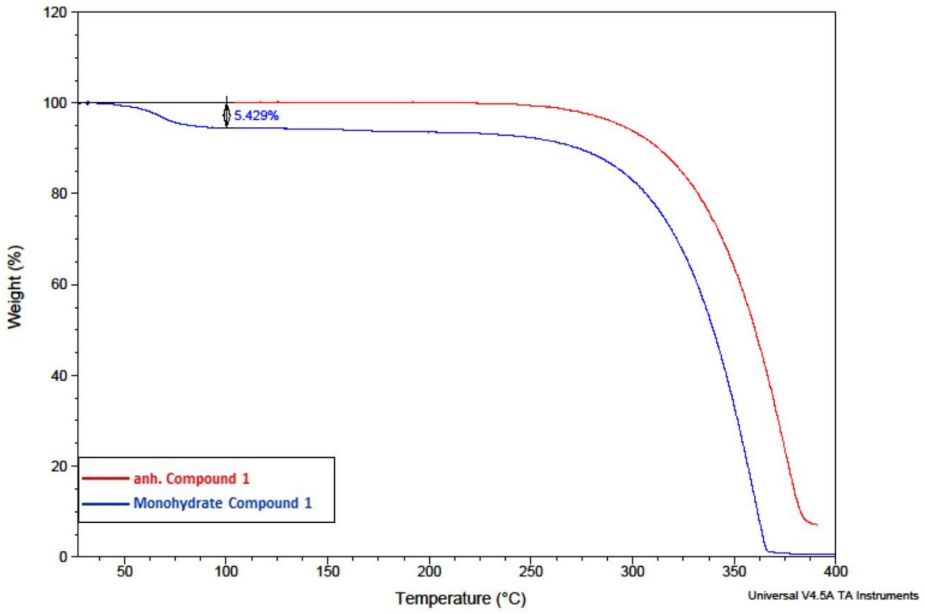

Figure S4. The TGA profile of monohydrate form of compound **1** obtained *via* ball-milling (blue) exhibits a weight loss of 5.4% at ~75 ˚C, corresponding to the water molecule present in the crystal structure of compound **1** compared to the TGA profile of anhydrate form of compound **1** obtained *via* SDG (red).

***N,N'*-Bis (4-pyridylmethylene)naphthalene-1,5-diamine (2).**

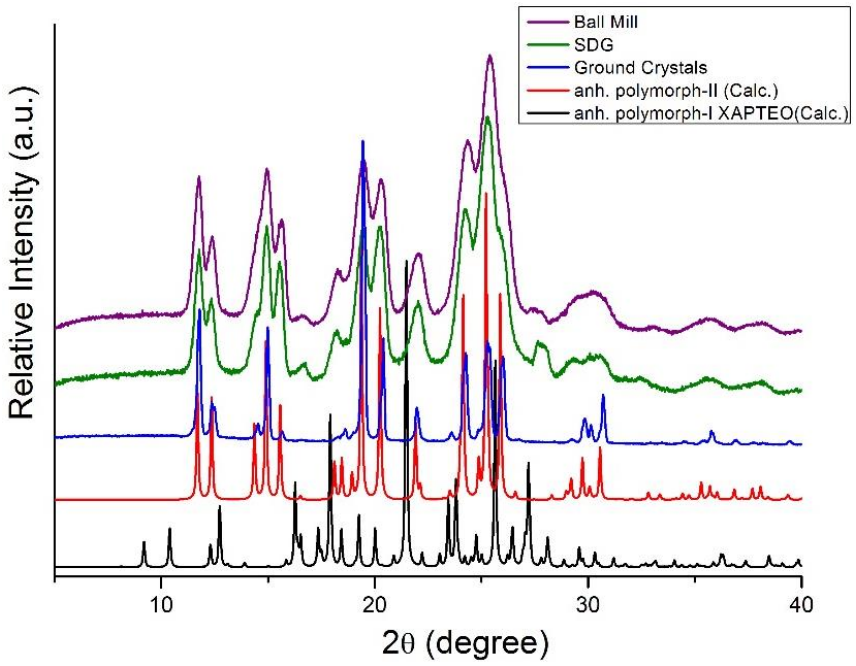

Figure S5. Calculated PXRD of previously reported polymorph-I (XAPTEO) (black), calculated PXRD generated from the single crystal structure of **2** (red) compared with the ground crystals of compound **2** (blue), compound **2** as-synthesized *via* SDG (green) and compound **2** as-synthesized *via* ball-milling (purple).

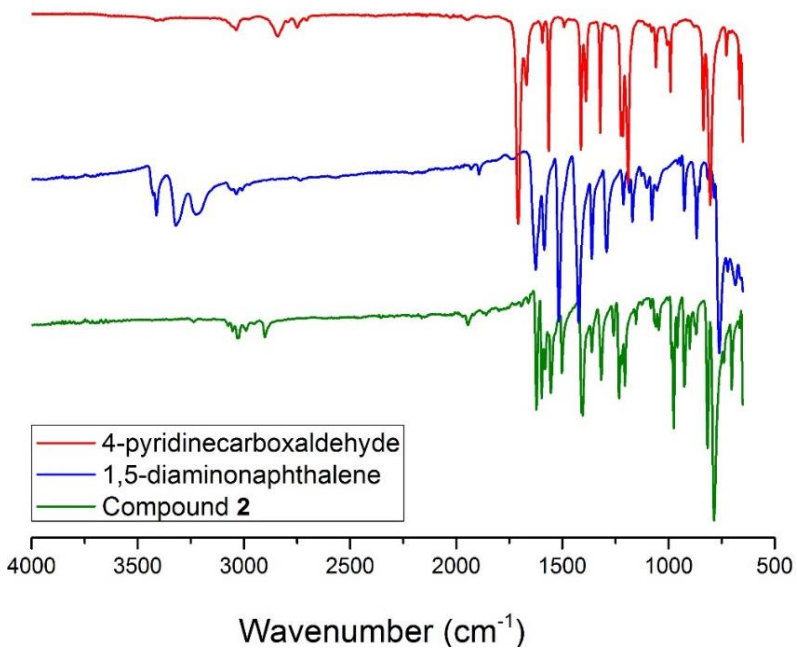

Figure S6. The FTIR spectra of compound **2** as-synthesized *via* SDG (green) compared with the starting materials (blue and red).

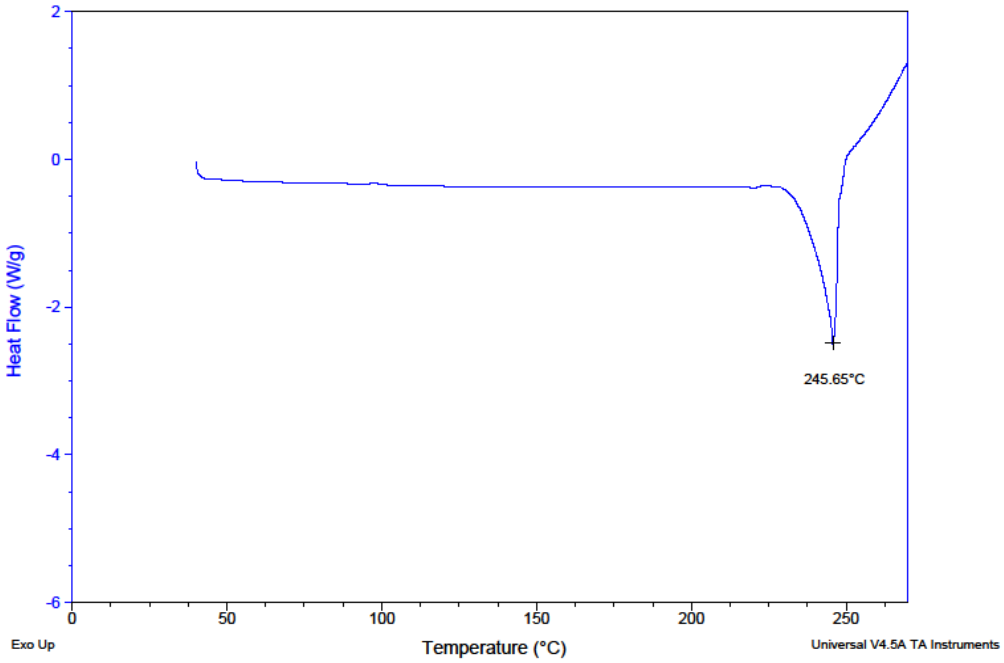

Figure S7. The DSC profile of compound **2** as-synthesized.

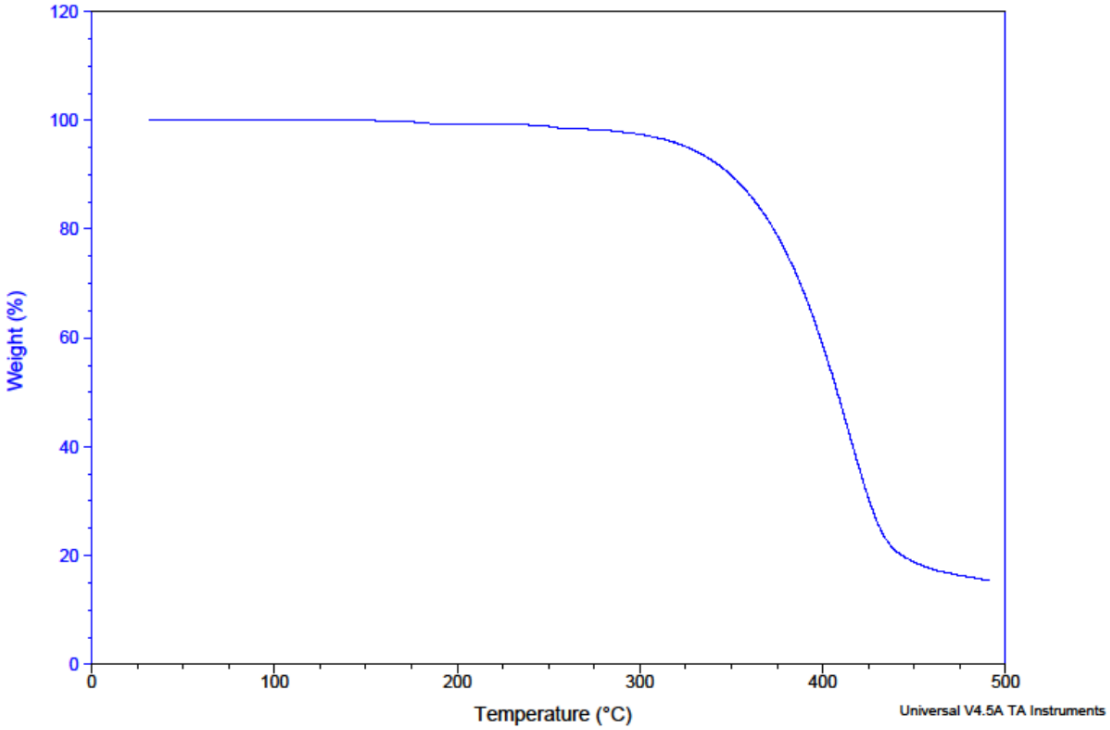

Figure S8. TGA profile of compound **2** as-synthesized.

***N*-(pyridin-4-ylmethylene)quinolin-5-amine (3).**

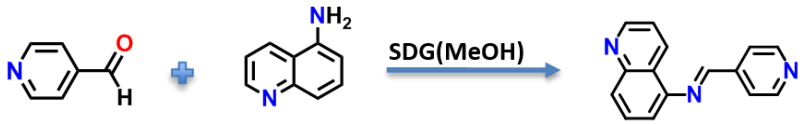

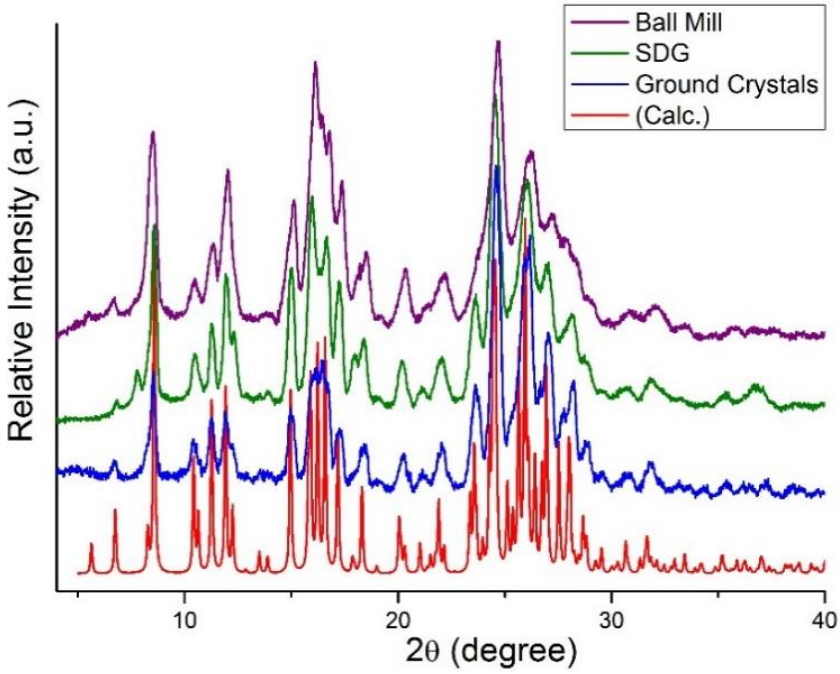

Figure S9. calculated PXRD generated from the single crystal structure of **3** (red) compared with the ground crystals of compound **3** (blue), compound **3** as-synthesized *via* SDG (green) and compound **3** as-synthesized *via* ball-milling (purple).

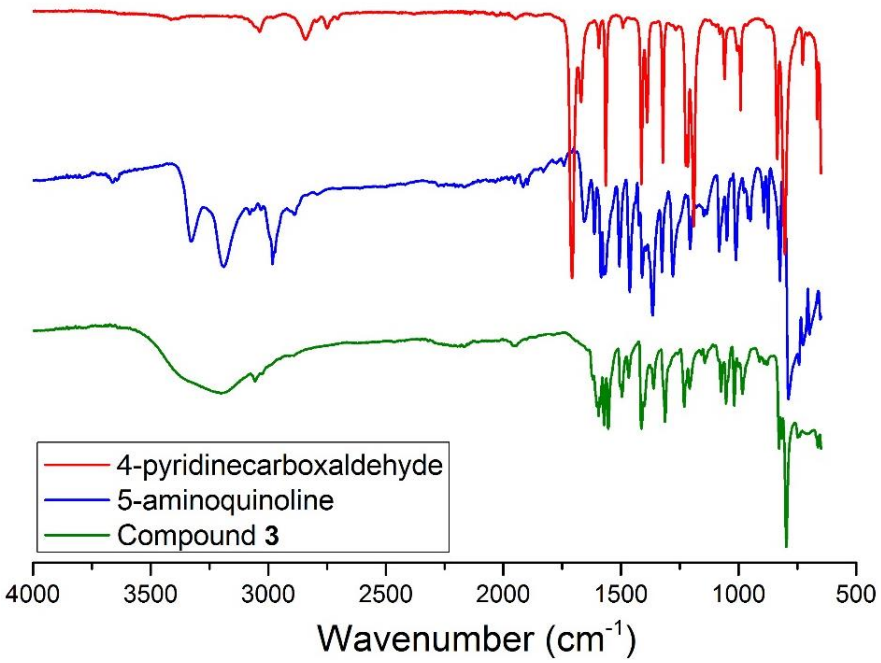

Figure S10. The FTIR spectra of compound **3** as-synthesized (green) compared to the starting materials (blue and red).

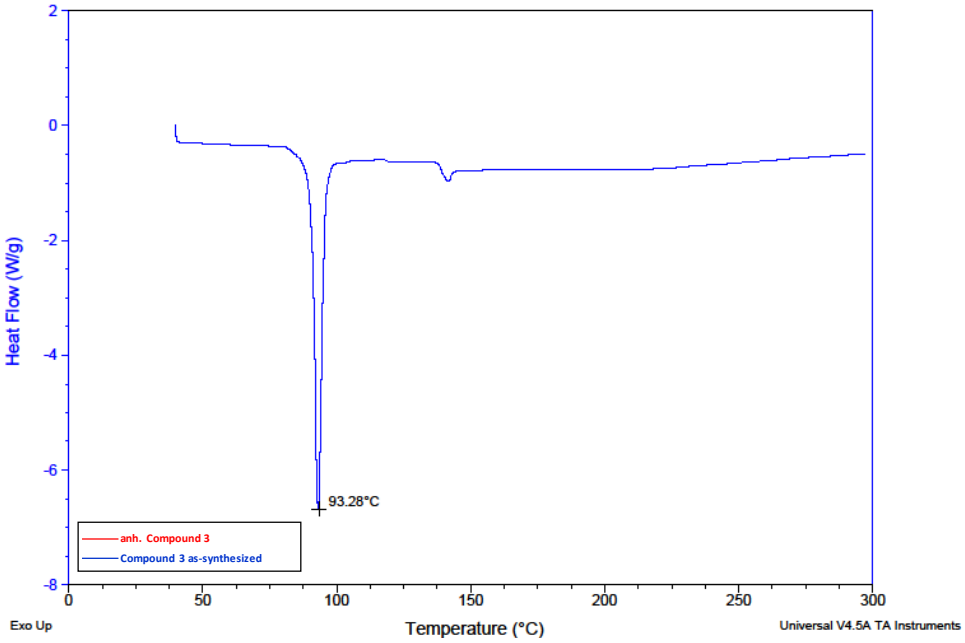

Figure S11. The DSC profile of compound **3** as-synthesized.

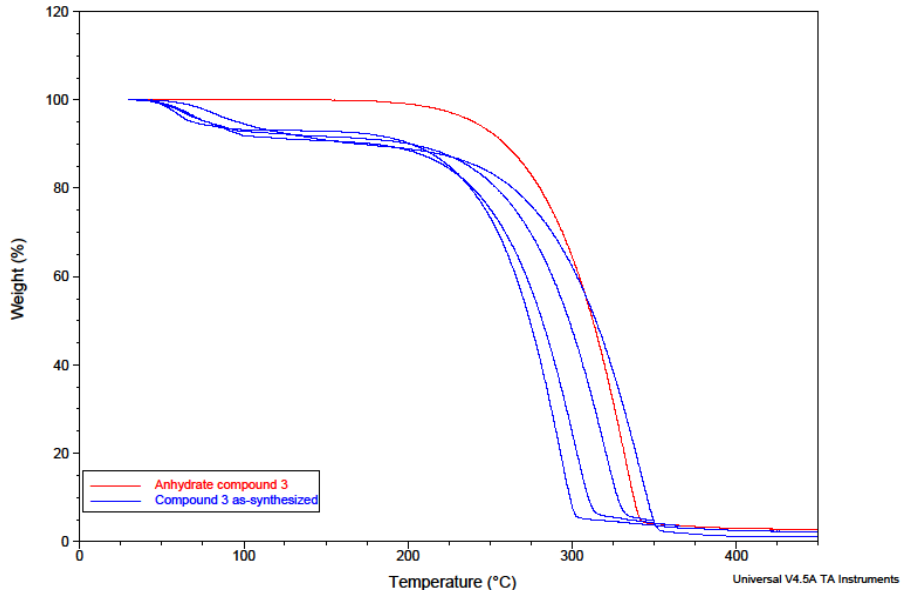

Figure S12. TGA profiles for the hydrated forms of compound **3** (blue) compared to anhydrate form obtained after heating compound **3** at 75˚C (red). Due to the partially channel character of the **3**.xH_2O and variable amount of water in the structure, TGA of as-synthesized compound **3** varies depending on the air exposure time (weight loss of 6.8%-9.1%). Therefore multiple TGA profiles were included in the graph (all marked in blue).

***N,N'*-4-(1H-imidazol-1-yl)-*N*-(pyridin-4-ylmethylene)aniline (4).**

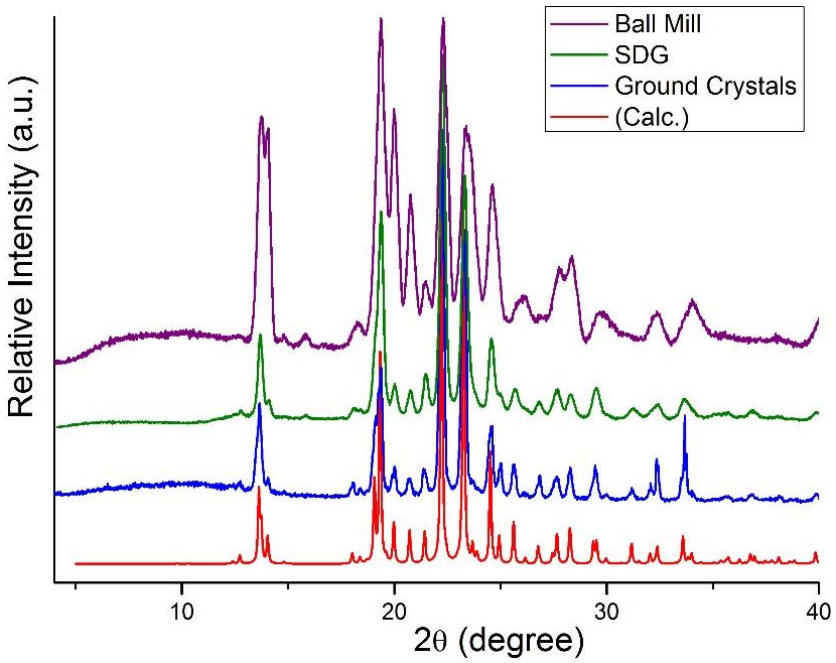

Figure S13. Calculated PXRD generated from the single crystal structure of **4** (red) compared with the ground crystals of **4** (blue), compound **4** as-synthesized *via* SDG (green) and compound **4** as-synthesized *via* ball-milling (purple).

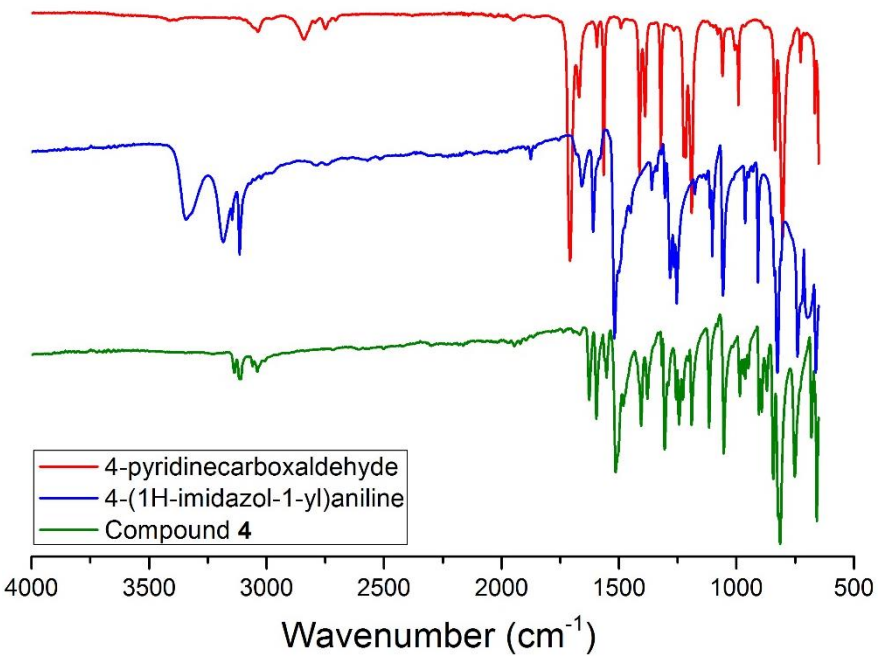

Figure S14. The FTIR spectra of compound **4** as-synthesized (green) compared with the starting materials (blue and red).

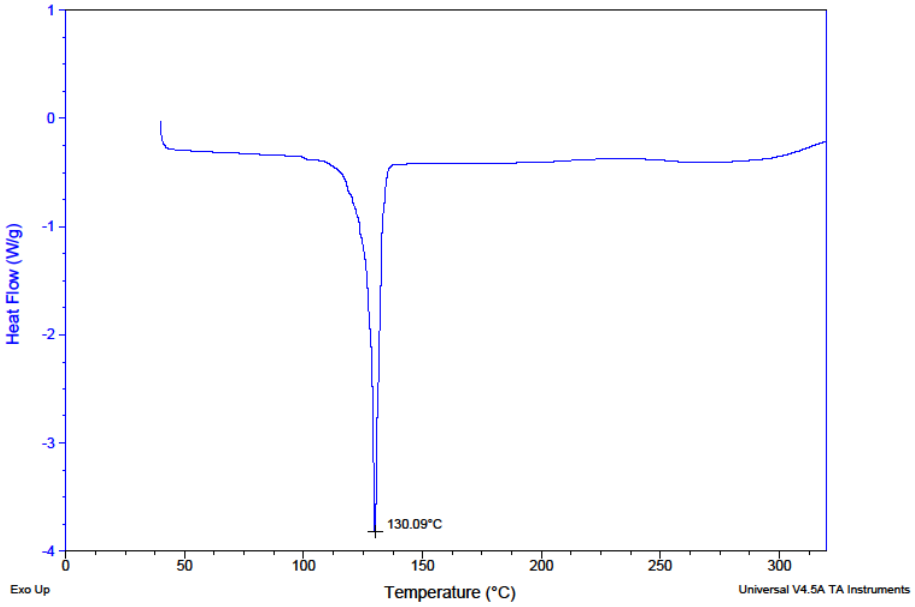

Figure S15. The DSC profile of compound **4** as-synthesized.

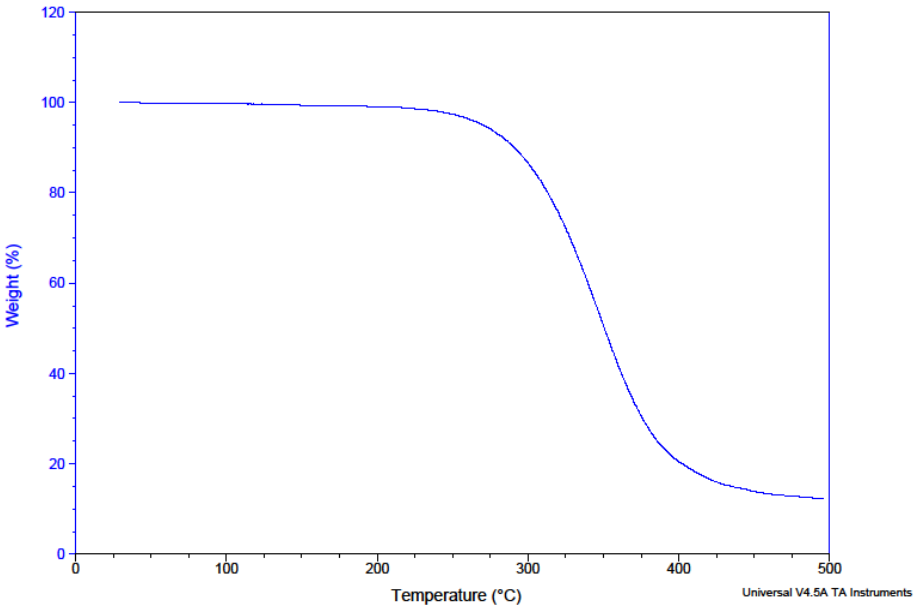

Figure S16. TGA profile for compound **4** as-synthesized.

N,N'-(1,4-phenylenebis(methan-1-yl-1-ylidene))bis(4-(1H-imidazol-1-yl)aniline) (5).

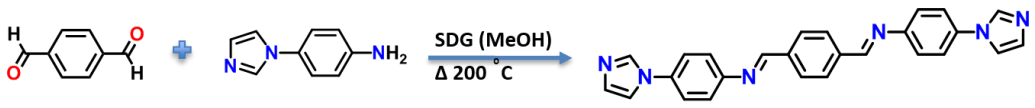

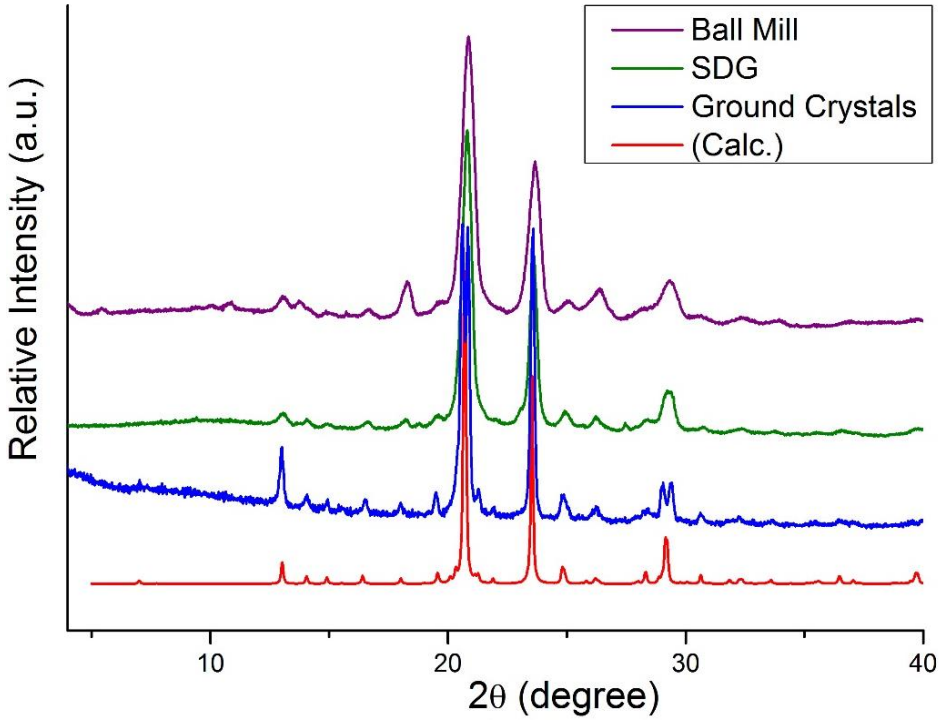

Figure S17. Calculated PXRD generated from the single crystal structure of **5** (red) compared with the ground crystals of compound **5** (blue), compound **5** as-synthesized *via* SDG (green) and compound **5** as-synthesized *via* ball-milling (purple).

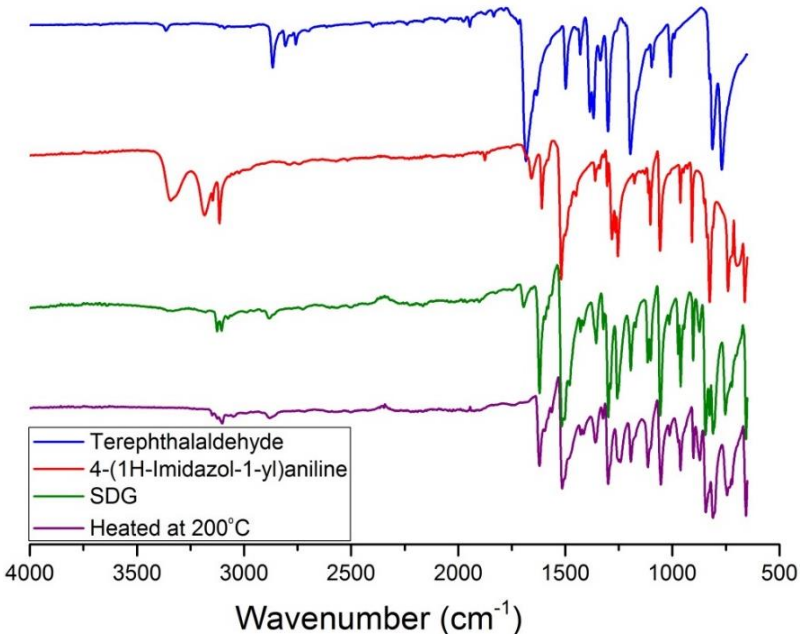

Figure S18. The FTIR spectra of compound **5** SDG (green) compared to the starting materials (blue and red) and after heating at 200˚C.

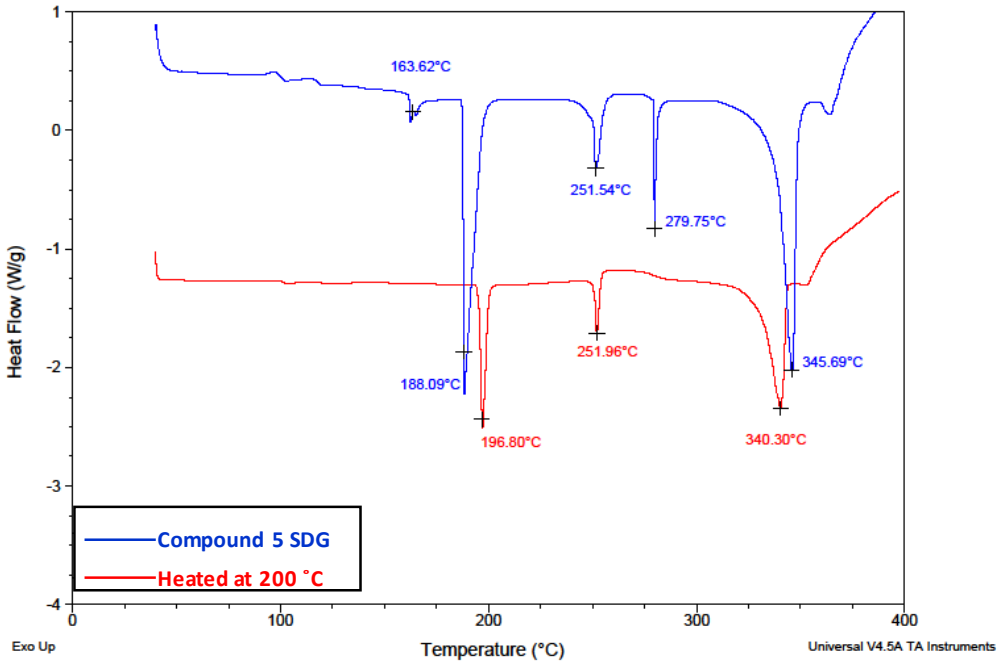

Figure S19. The DSC profiles of compound **5** SDG (blue) and after heating at 200˚C (red).

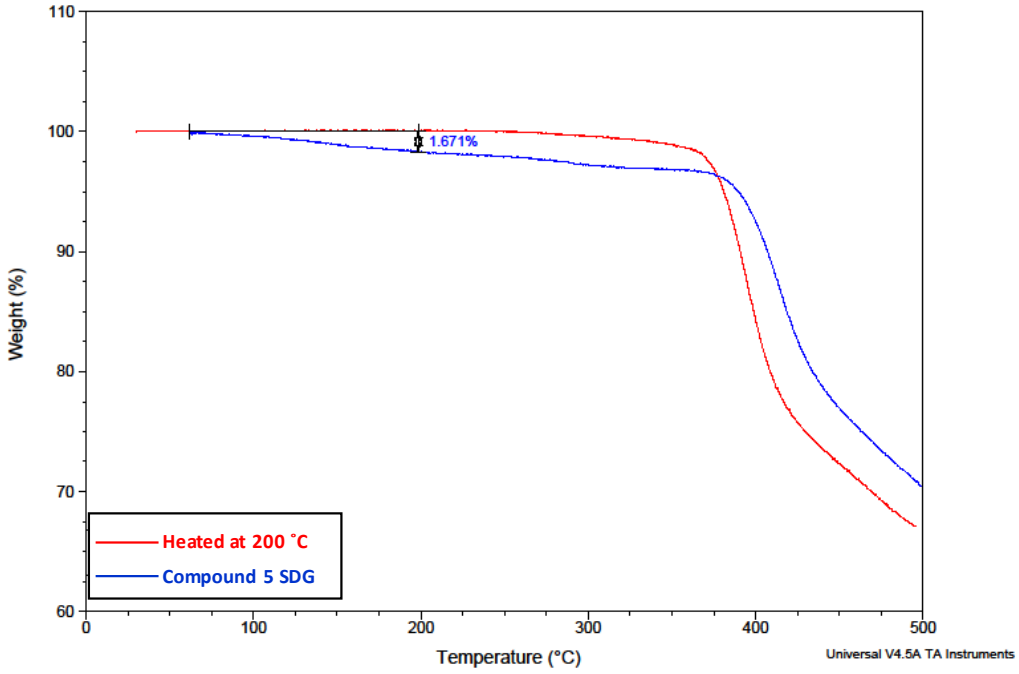

Figure S20. TGA profiles for compound **5**. SDG (blue) and after heating at 200˚C (red).

N,N'-(1,4-phenylenebis(methan-1-yl-1-ylidene))diquinolin-5-amine (6).

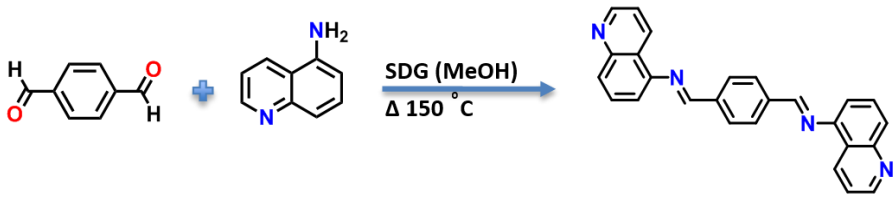

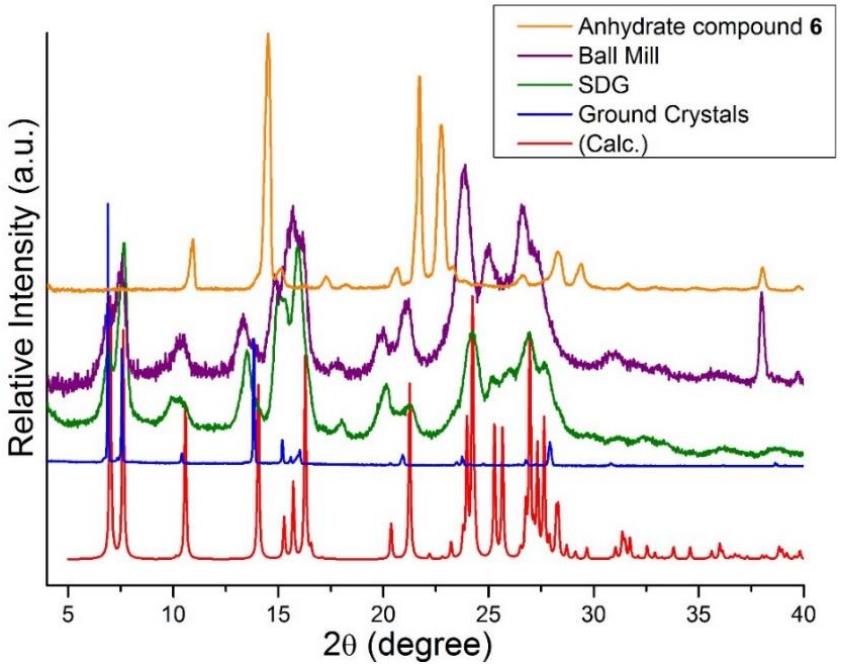

Figure S21. Calculated PXRD of **6** generated from the single crystal structure **6** (red) compared to ground crystals of compound **6** (blue), compound **6** as-synthesized *via* SDG (green), compound **6** as-synthesized *via* ball-milling (purple) and anhydrate form of compound **6** obtained after heating at 150˚C (orange).

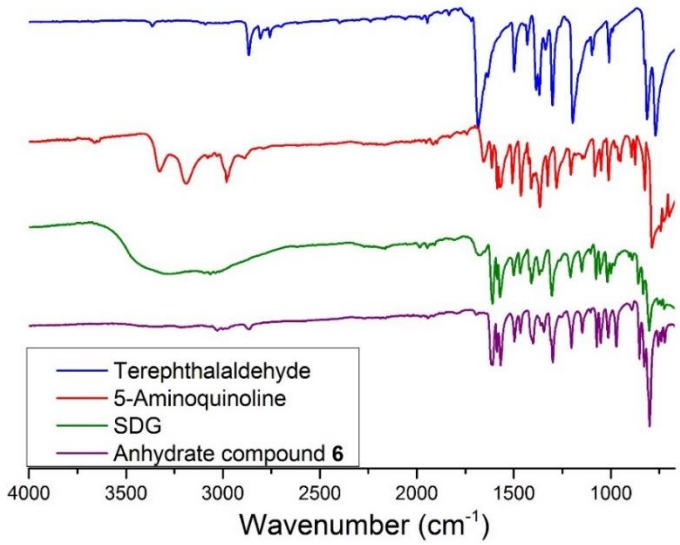

Figure S22. The FTIR spectra of compound **6** SDG (green) compared to the starting materials (blue and red) and the anhydrate form of compound **6** obtained after heating at 150 ˚C.

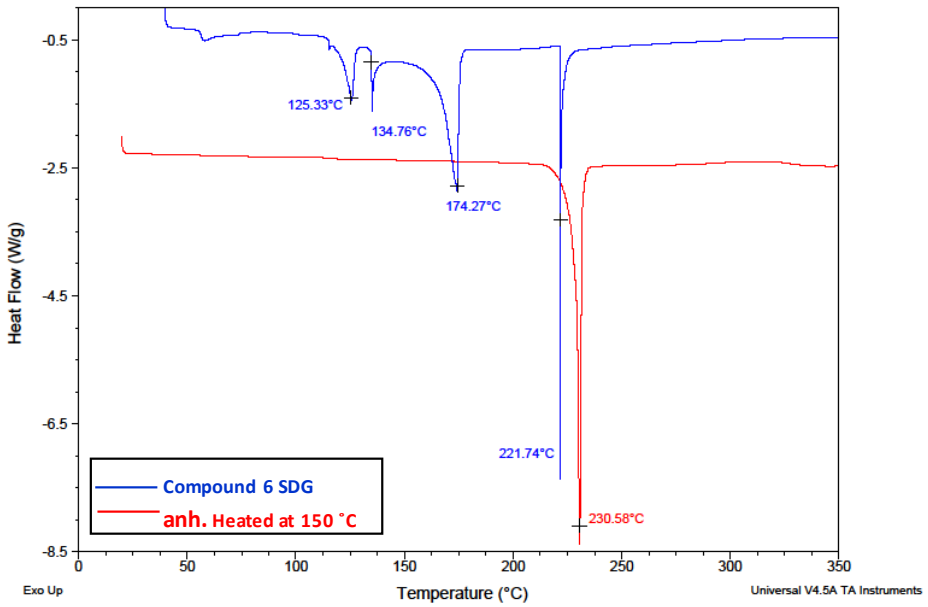

Figure S23. The DSC profiles of anhydrous form of compound **6** obtained after heating at 150˚C (red) compared to the SDG (blue).

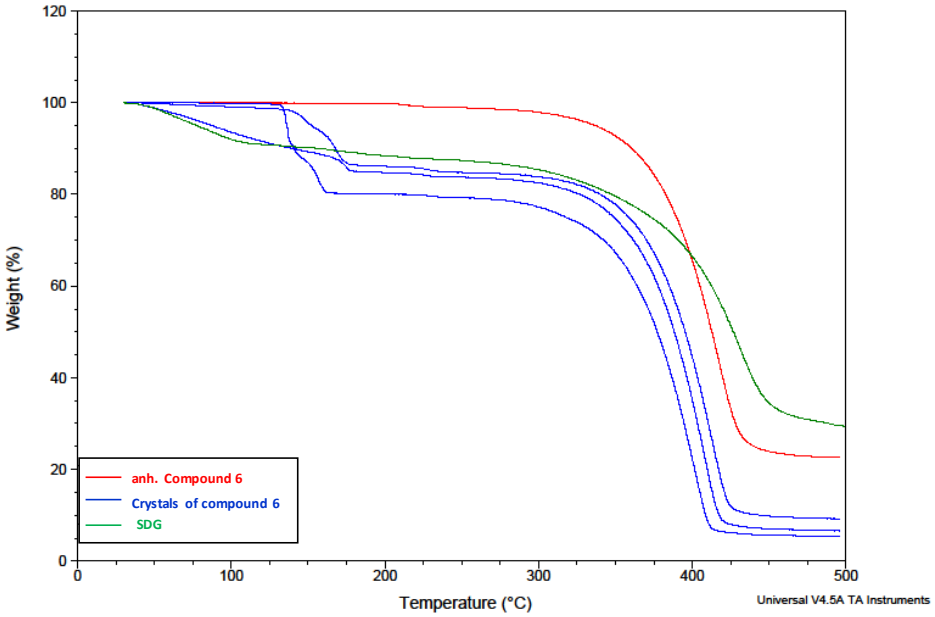

Figure S24. TGA profiles for the different batches of crystals of heterosolvate form of compound **6** (blue) compared to the SDG (green) and anhydrate form, obtained after heating compound **6** at 150˚C (red). The variable TGA profiles indicate changing ratio of methanol and water in the crystal structure.

N,N'-(1,4-phenylenebis(methan-1-yl-1-ylidene))dipyridine-4-amine (7).

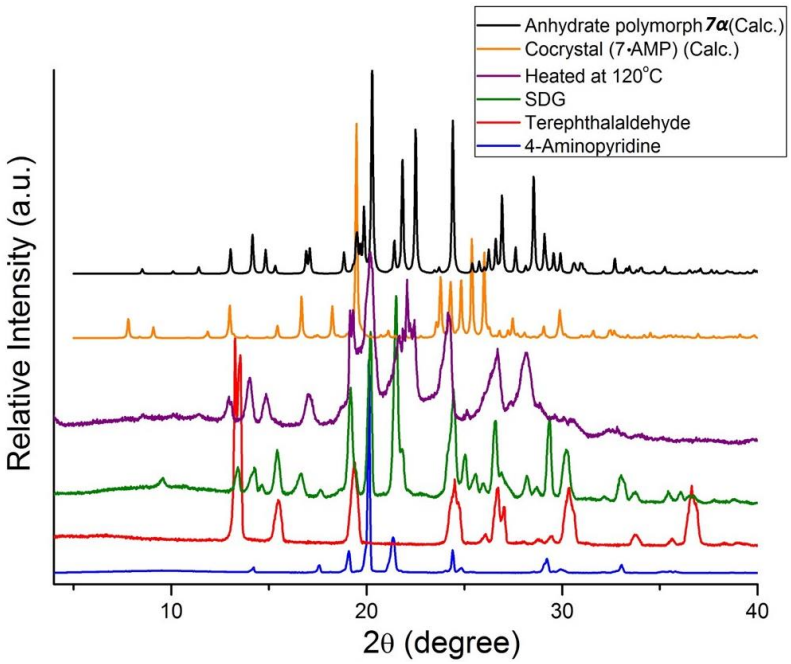

Figure S25. PXRD comparison of starting materials (blue and red), SDG (green), after heat (purple), cocrystal of **7** and 4-aminopyridine (**7•AMP**) (orange) and polymorph ***7α*** (black). PXRD of solvent-drop grind sample (SDG) reveals presence of unreacted starting materials, while PXRD of the heated sample matches the mixture of cocrystal (**7•AMP**) and anhydrous polymorph ***7α***.

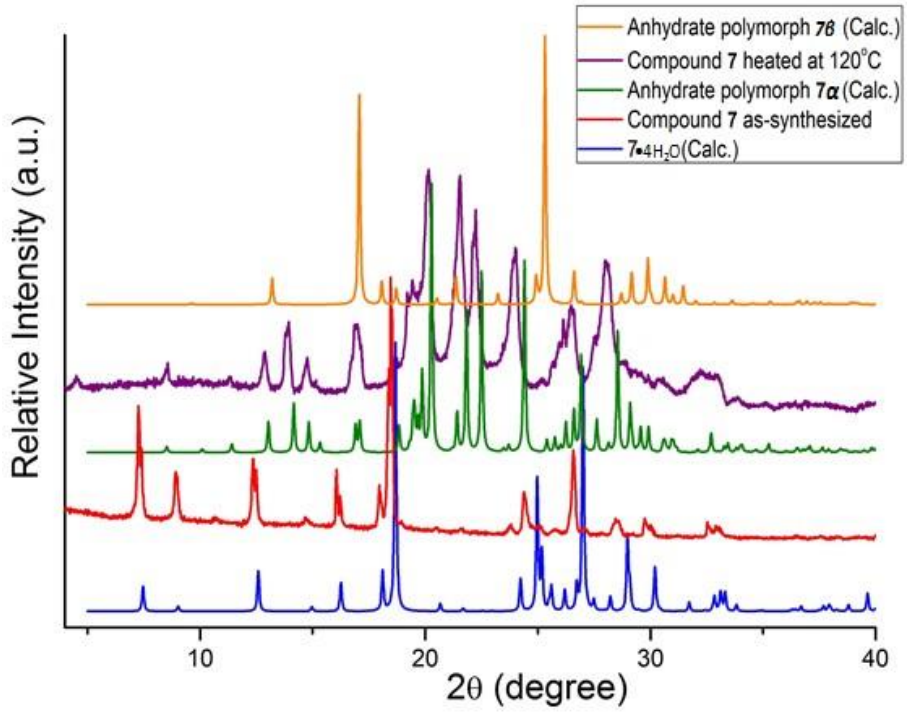

Figure S26. PXRD patterns calculated for compound **7** polymorphs ***α*** (green) and ***β*** (orange), and hydrate of compound **7** (blue), as well as experimental PXRD of as synthesized sample (red) and sample after heating at 120˚C (purple). PXRD of as-synthesized sample matches PXRD calculated for hydrate of compound **7** (**7**•4H_2O), while PXRD of heated sample matches PXRD calculated for polymorph ***α*** of compound **7**.

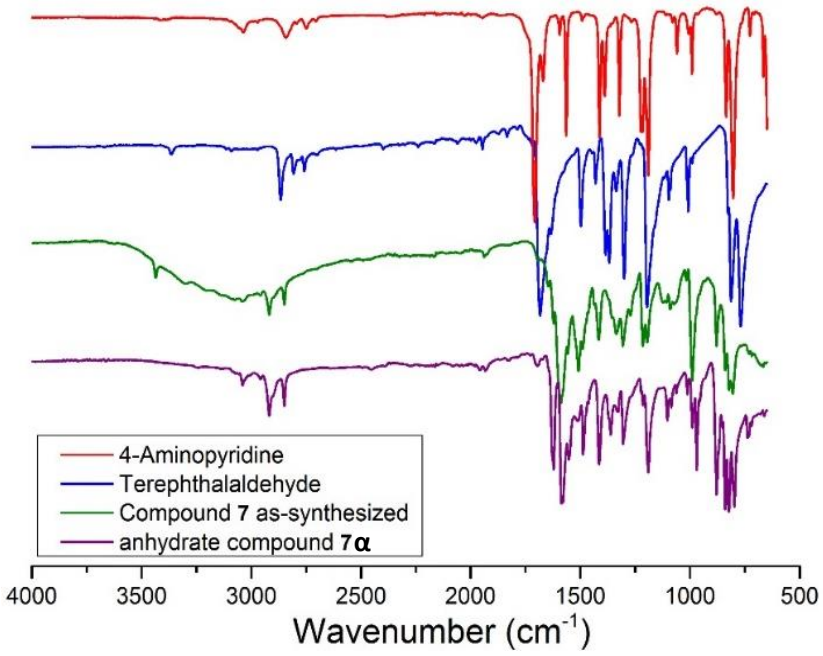

Figure S27. The FTIR spectra of as-synthesized hydrate of compound **7** (**7**•4H_2O) (green) compared to the starting materials (blue and red) and anhydrous form (**7*α***) obtained after heating at 120˚C (purple).

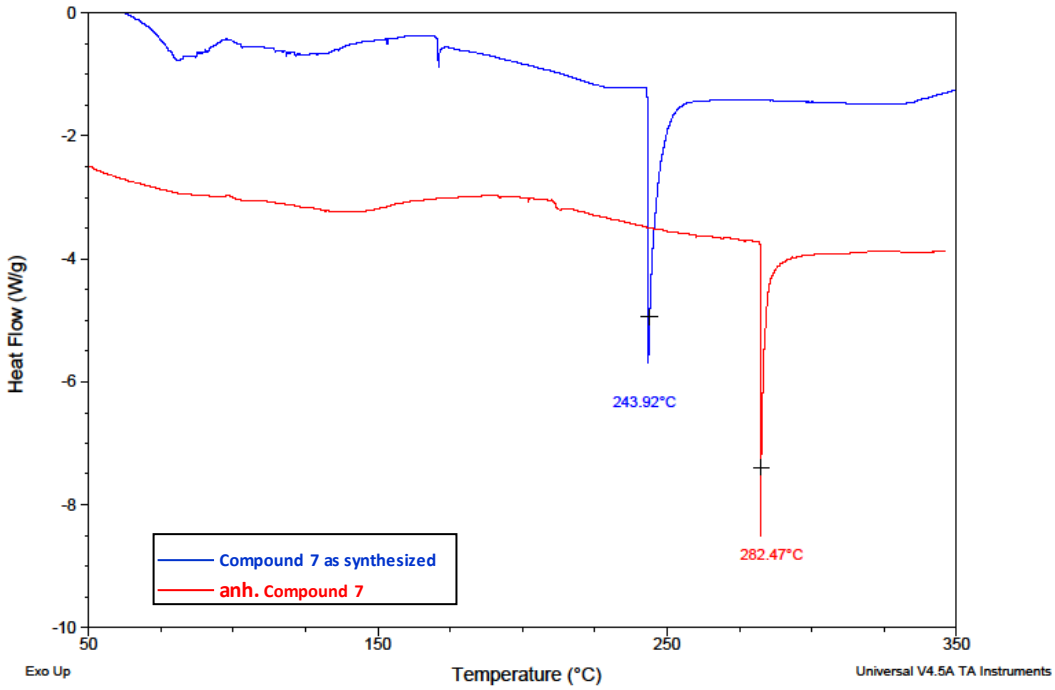

Figure S28. The DSC profiles of compound **7** as-synthesized (**7**•4H_2O) (blue) and anhydrous form of **7** (**7*α***) obtained after heating (red).

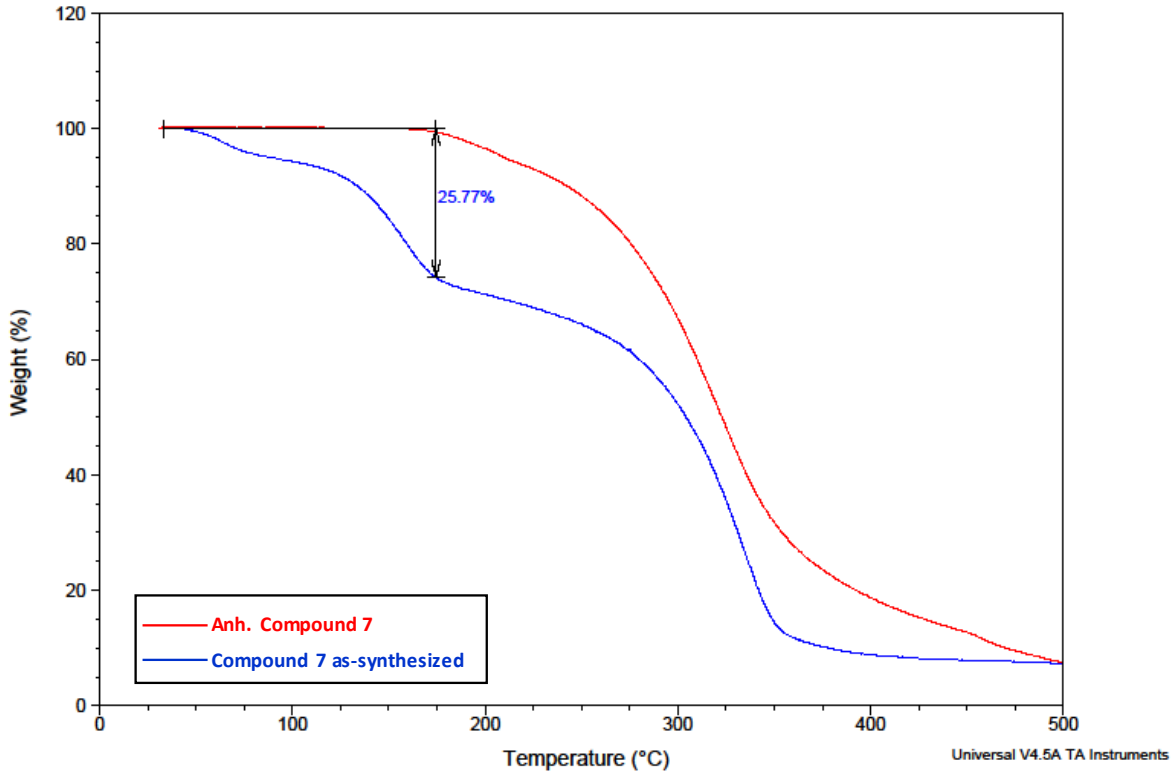

Figure S29. TGA profiles for compound **7** as synthesized (**7**•4H_2O) (blue) and anhydrous form of **7** (**7*α***) obtained after heating at 120˚C (red)

4-((4-(1H-imidazol-1-yl)phenylimino)methyl)benzoic acid (8).

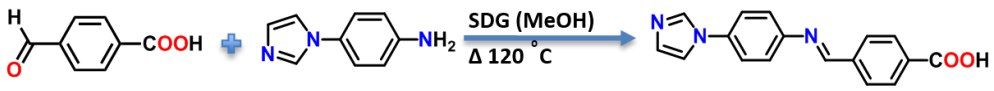

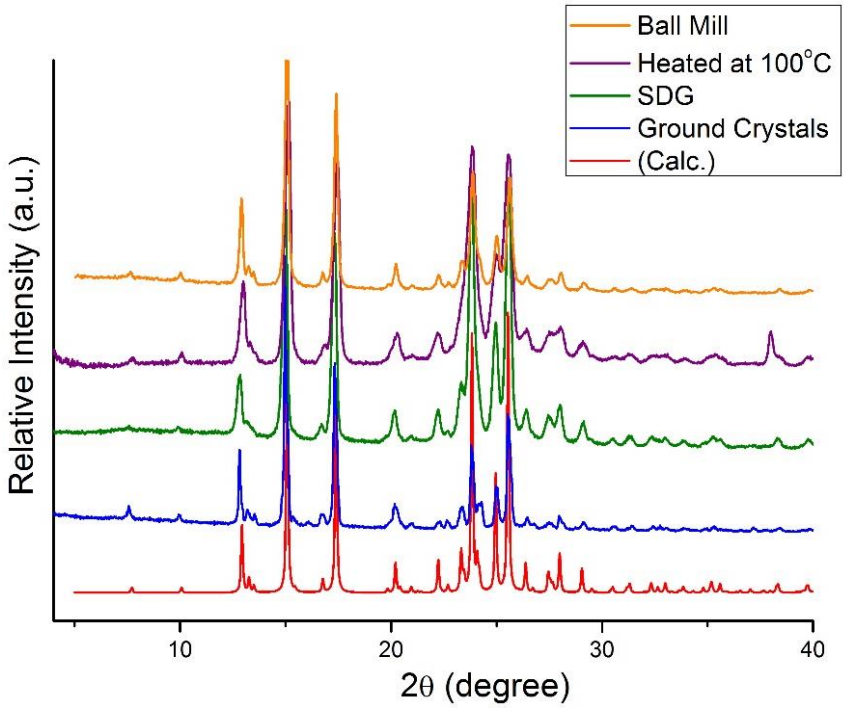

Figure S30. Calculated PXRD of **8** generated from the single crystal structure of **8** (red) compared to the ground crystals of compound **8** (blue), compound **8** as-synthesized *via* SDG (green), the heated sample at 100˚C (orange) and compound **8** as-synthesized *via* ball-milling (purple).

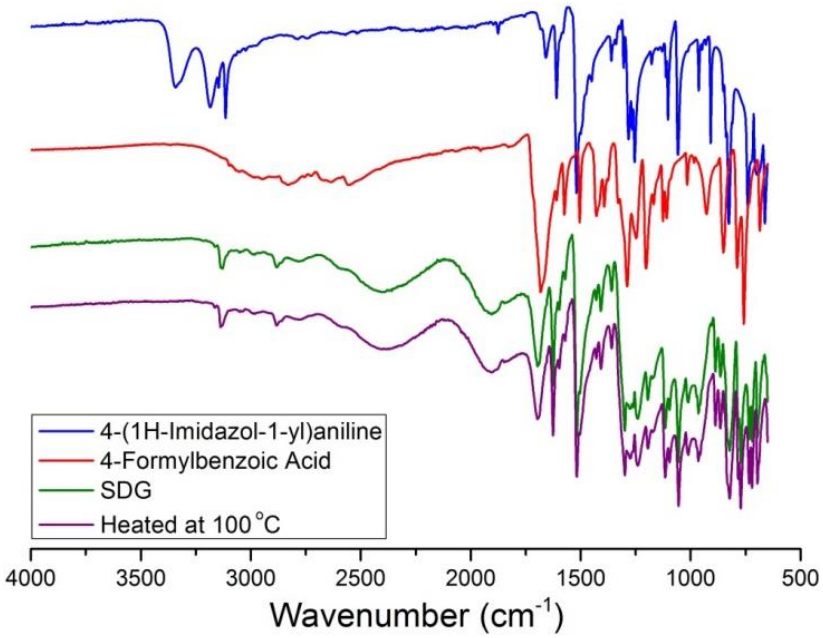

Figure S31. The FTIR spectra of compound **8** SDG (green) compared to the starting materials (blue and red) and after heating at 100˚C.

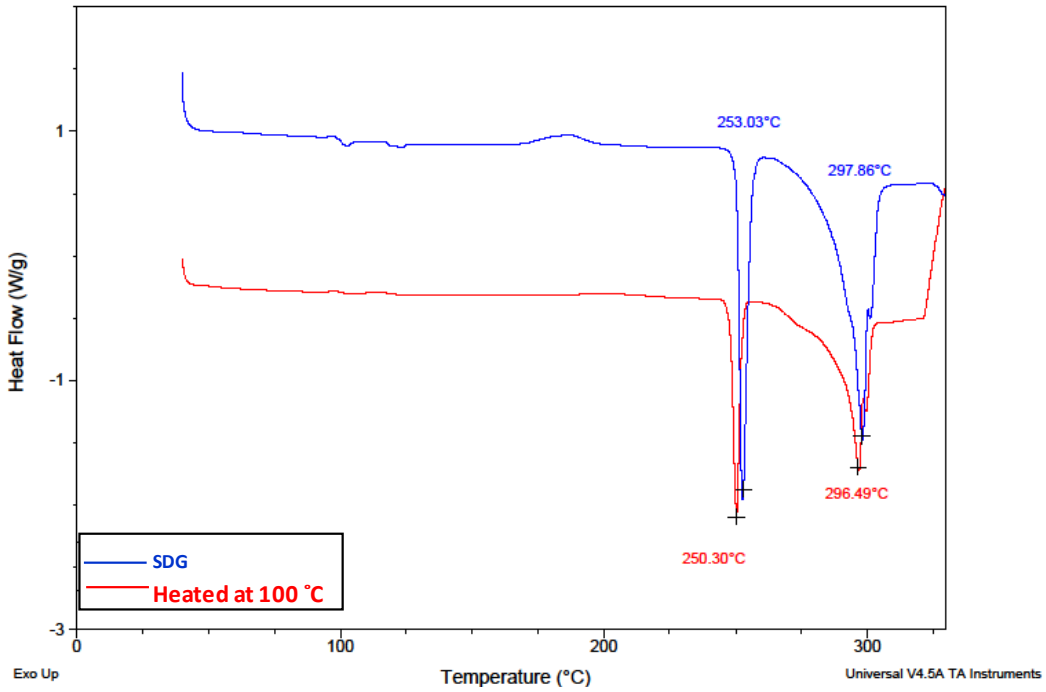

Figure S32. The DSC profiles comparison of compound **8** SDG (blue) and after heating at 100˚C (red).

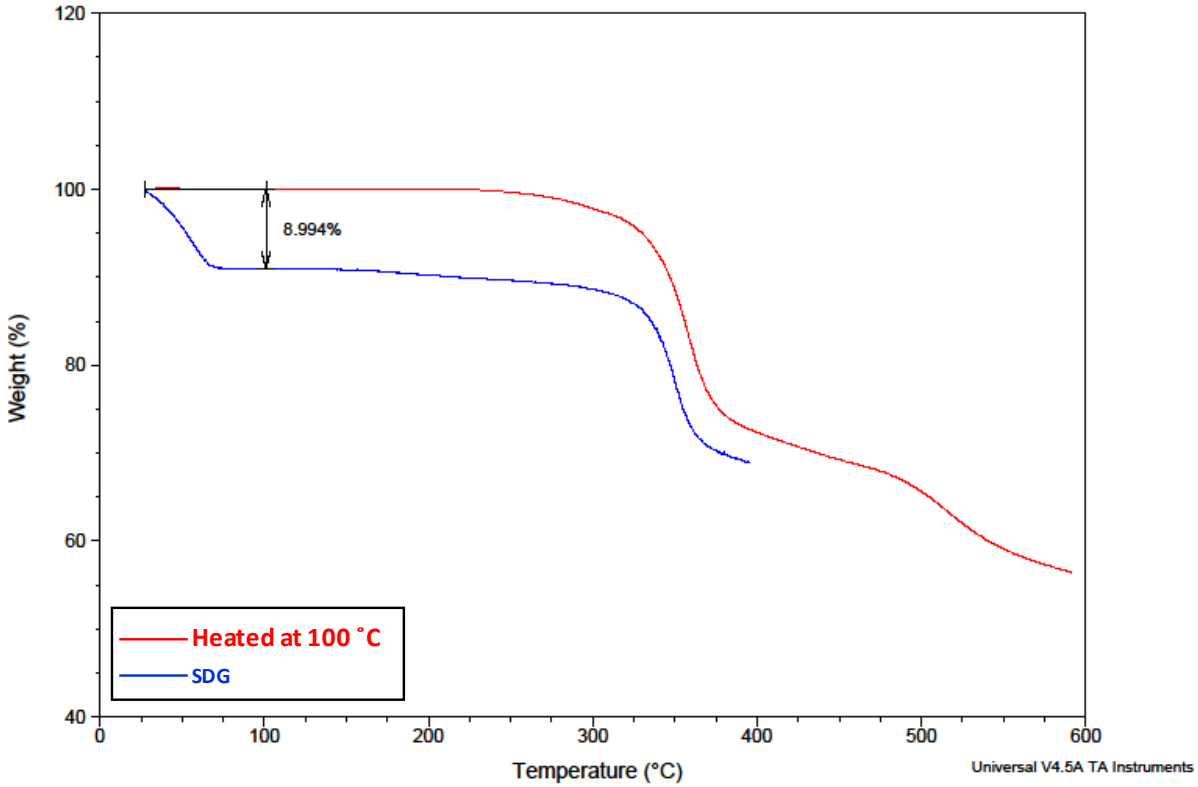

Figure S33. TGA profiles for compound **8**. SDG (blue) and after heat 100˚C (red).

Table S1. List of dihedral and torsion angles and bond distances observed in the crystal structures of compounds **1-8**.

Compound	Structure code	Torsion angles between aryl rings (°)			Torsion Angles about imine fragment (°)		Bond Distances In The Imine Fragment (Å)		
		$\angle_{AB}$	$\angle_{BC}$	$\angle_{AC}$	C^1-C^2-C^3-N^4	C^3-N^4-C^5-C^6	C–C	C=N	C – N
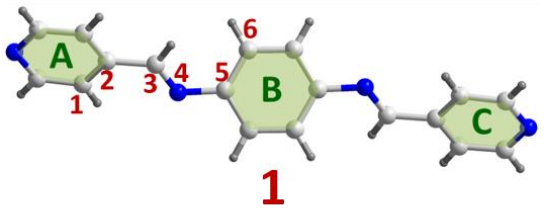 1	**PEXXEW**	53.29, 58.10[a]	-	-	9.98(6), 6.10(6)[a]	47.61(5), 47.87(5)[a]	1.466(1), 1.474(1)[a]	1.253(1), 1.255(1)[a]	1.414(1), 1.420(1)[a]
	OXUHIA02	52.49	-	-	8.74(1)	42.87(1)	1.475(1)	1.263(1)	1.424(1)
	HIRLUQ	24.96	43.79	68.60	4.64(2), 4.54(2)[b]	28.72(2), 40.58(2)[b]	1.476(1), 1.465(1)[b]	1.259(1), 1.250(1)[b]	1.414(1), 1.433(1)[b]
	1 (Monohydrate)	24.43	46.21	70.46	5.47(18), 2.38(19)[b]	29.34(17), 43.32(16)[b]	1.467(2), 1.470(2)[b]	1.273(2), 1.272(1)[b]	1.417(2), 1.416(2)[b]
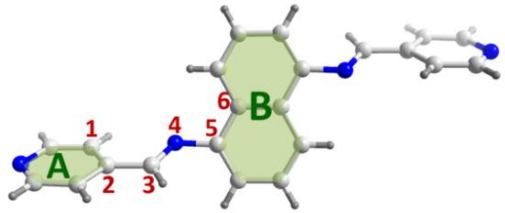 2	**New Polymorph**	62.52	-	-	13.40(1)	132.18(1)	1.468(1)	1.265(1)	1.416(1)
	XAPTEO	57.52, 53.85[a]	-	-	1.14(1), 6.78(1)[a]	129.05(1), 133.32(1)[a]	1.469(1), 1.471(1)[a]	1.268(1), 1.274(1)[a]	1.414(1), 1.416(1)

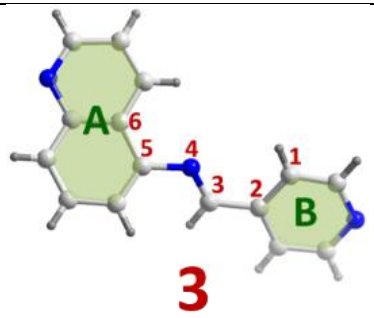	37.99, 41.55[a]	-	-	0.40(1), 0.78(1)[a]	142.06(1), 144.19(1)[a]	1.474(1), 1.474(1)	1.275(1), 1.273(1)	1.418(1), 1.417(1)
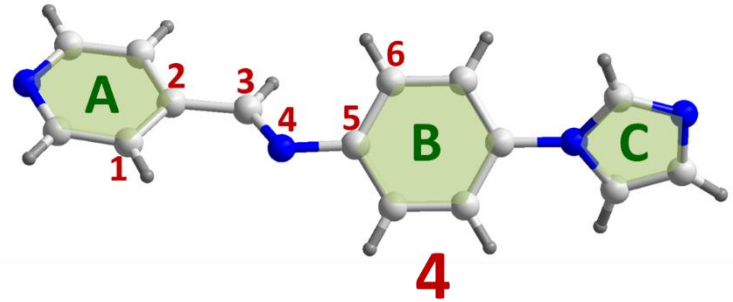	40.61	39.15	79.75	4.86(1)	45.39(1)	1.469(1)	1.261(1)	1.422(1)
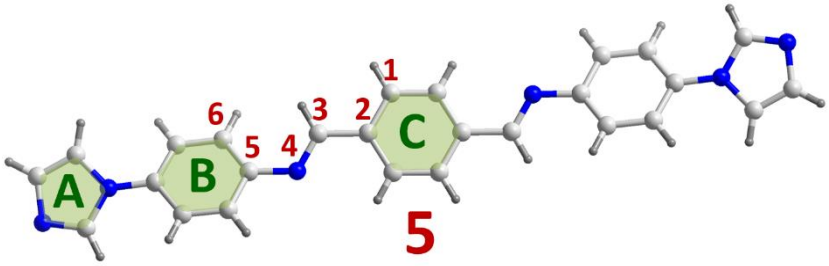	25.80, 24.62[a]	18.32, 16.00[a]	15.35, 10.86[a]	167.70(4), 170.88(5)[a]	28.21(8), 24.41(8)[a]	1.469(1), 1.474(1)[a]	1.270(1), 1.258(1)[a]	1.427(1), 1.420(1)[a]

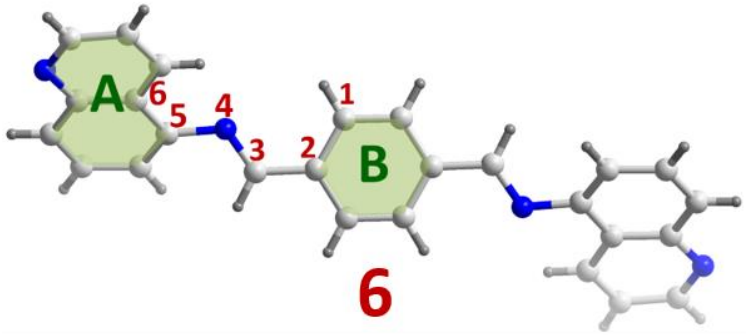		42.51	-	-	1.65(1)	142.55(1)	1.466(1)	1.278(1)	1.416(1)
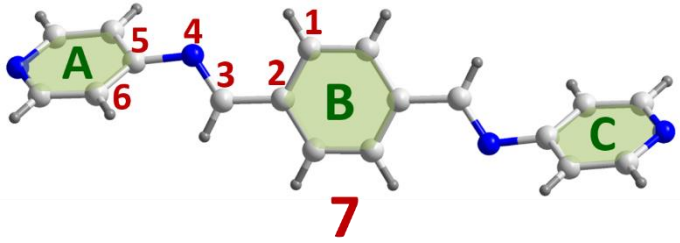	**7*α***	63.65, 46.62[a]	-	-	8.44(1), 6.24(1)[a]	56.20(1), 40.23(1)[a]	1.467(1), 1.469(1)[a]	1.273(1), 1.274(1)[a]	1.417(1), 1.419(1)[a]
	7*β*	48.57	-	-	5.19(1)	42.46(1)	1.471(1)	1.278(1)	1.420(1)
	7•AMP	49.49, 47.89[c]	54.38	-	8.94(1), 3.61(1)[b] 3.13(1)[c]	45.26(1), 46.26(1)[b] 44.41(1)[c]	1.465(1), 1.470(1)[b] 1.466(1)[c]	1.275(1), 1.273(1)[b] 1.275(1)[c]	1.415(1), 1.414(1)[b] 1.412(1)[c]
	7•4H_2O	41.48	-	-	3.29(1)	45.18(1)	1.465(1)	1.273(1)	1.413(1)

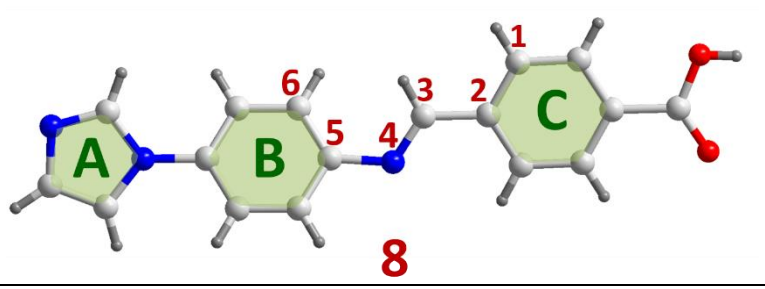	28.11	31.09	3.32	179.92(1)	31.36(1)	1.457(1)	1.260(1)	1.416(1)

[a]For these crystal structures, molecules of respective compounds lie on a centre of symmetry. However, there are two halves of crystallographically independent molecules in the asymmetric unit, therefore two sets of values are listed in the table.

[b]In this crystal structure, the molecule lies on a general position; therefore, it is non-symmetrical and therefore two sets of values are included in the table.

[c]In this crystal structure, there is 1.5 molecules of **7** in the asymmetric unit, therefore three values are reported for discussed torsion angles and bond distances, and two values are listed for dihedral angle between rings A and B.

Table S2. List of dihedral and torsion angles and bond distances observed in the crystal structures of **sql-5-Ni-4i**.

Compound	Torsion angles between aryl rings (°)									
	∠AB	∠AC	∠AD	∠AE	∠BC	∠BD	∠BE	∠CD	∠CE	∠DE
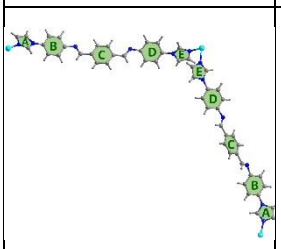	32.60, 12.14 [d]	30.46, 20.82 [d]	57.31, 14.02[d]	88.09, 51.54[d]	12.91, 32.95[d]	24.72, 7.52[d]	59.59, 39.68[d]	31.11, 33.70[d]	66.26, 72.19[d]	35.40, 38.73[d]

Torsion Angles about imine fragment (°)		Bond Distances In The Imine Fragment (Å)		
C^1-C^2-C^3-N^4	C^3-N^4-C^5-C^6	C–C	C=N	C – N
172.73(1), 169.84(1) 178.18(1)[d], 4.26(1)[d]	157.00(1), 40.89(1) 166.68(1)[d], 34.11(1)[d]	1.474(1), 1.466(1) 1.473(1)[d], 1.461(1)[d]	1.271(1), 1.275(1) 1.238(1)[d], 1.260(1)[d]	1.414(1), 1.419(1) 1.421(1)[d], 1.424(1)[d]

[d]The asymmetric part of the unit-cell contains two ligand molecules coordinated to Ni^{2+} cation; therefore, values of dihedral and torsion angles, as well as bond lengths for both ligands were included in the table.

Crystallization of Single-Crystals of Compounds 1-8

Compound 1. Yellow needle shaped crystals of **1** were isolated by slow evaporation of **1** in (20 mg, 0.07 mmol) in 3 mL of MeOH over a period of 5 d (95% yield).

Compound 2. Yellow plate crystals were isolated by slow evaporation of a solution of **2** (50 mg, 0.15 mmol) in 4 mL of MeOH/$CHCl_3$ (1:1 *v/v*) over a period of 6 d (97% yield).

Compound 3. Yellow needle-shaped crystals of **3** were isolated by slow evaporation of 3 (50 mg, 0.19 mmol) in 4.5 mL of MeCN over a period of 4 d (96% yield).

Compound 4. Yellow crystals of **4** were isolated upon slow evaporation of a solution of 4 (20 mg, 0.08 mmol) in 2.5 mL of DMF/MeOH (1:4 *v/v*) mixture over a period of 2 weeks (96% yield).

Compound 5. Yellow needle-shaped crystals were isolated by slow evaporation of **5** (20 mg, 0.04 mmol) in 4 mL of MeOH/$CHCl_3$ (1:1 *v/v*) mixture over a period of 6 d (97% yield).

Compound 6. Deep yellow needles were isolated by slow evaporation of **6** (20 mg, 0.05 mmol) in 4 mL MeOH/$CHCl_3$ (1:1 *v/v*) mixture over a period of 5 d (97% yield).

Compound 7. Needle-shaped crystals were isolated upon heating the ground mixture of the starting materials (32 mg) at 120 ˚C for 1 h. SCXRD experiments revealed that these crystals were a mixture of ***7α*** and **7•AMP**. These crystals (40 mg) were dissolved in various solvents and subjected to crystallization via slow evaporation. Slow evaporation using EtOH led to isolation of pure ***7β*** while using acetonitrile or acetone led to **7**•$4H_2O$ (92% yield based on starting materials). Pure ***7α*** was isolated by heating crystals of **7**•$4H_2O$ at 120 ˚C for 1 h (Figure S29).

Compound 8. Pale yellow plate-shaped crystals were obtained by slow evaporation of **8** (30 mg, 0.1 mmol) in 8 mL of MeOH/$CHCl_3$ (1:1 *v/v*) mixture over a period of 5 d (95% yield).

Table S3. Single crystal X-ray crystallographic details of compounds **1-8**.

Compound	**2**	**3**	**4**	**5**	**6**	***7α***	***7β***	**7•AMP**	**7•4H_2O**	**8**
Formula	$C_{22}H_{16}N_4$	$C_{15}H_{11}N_3$•xH_2O	$C_{15}H_{12}N_4$	$C_{26}H_{20}N_6$	$C_{26}H_{18}N_4$·1.4H_2O·0.6CH_4O	$C_{18}H_{14}N_4$	$C_{18}H_{14}N_4$	$3C_{18}H_{14}N_4$·2$C_5H_6N_2$	$C_{18}H_{14}N_4$·4H_2O	$C_{17}H_{13}N_3O_2$
M(g·mol^{-1})	336.39	251.28[a]	248.29	416.48	429.49	286.33	286.33	1047.23	343.98	291.30
T(K)	298(2)	100(2)	273(2)	101(2)	100(2)	100(2)	100(2)	100(2)	100(2)	298(2)
λ(Å)	0.71073	1.54178	0.71073	1.54178	1.54178	1.54178	1.54178	1.54178	0.71073	1.54178
Crystal System	Monoclinic	Orthorhombic	Triclinic	Triclinic	Monoclinic	Triclinic	Monoclinic	Monoclinic	Monoclinic	Monoclinic
Space Group	$P2_1/n$	$Pna2_1$	$P\bar{1}$	$P\bar{1}$	$P2_1/c$	$P\bar{1}$	$P2_1/c$	$P2_1/c$	$P2_1/c$	$P2_1/c$
Z/*Z*′	2/0.5	8/2	2/1	2/1	2/0.5	2/1	2/0.5	2/0.5	2/0.5	4/1
Unit-cell parameters (Å/°):										
a	8.3858(5)	41.0121(18)	8.0119(4)	5.8872(16)	12.6746(3)	7.5390(2)	3.83390(10)	9.8761(3)	11.9710(5)	4.5880(3)
b	9.6049(6)	16.9045(7)	9.0076(4)	13.583(3)	3.86570(10)	9.7461(3)	9.8095(3)	11.8796(3)	3.7363(2)	13.5933(7)
c	11.1997(7)	3.7988(2)	9.8727(5)	13.613(3)	23.1653(5)	10.7781(3)	18.3519(5)	22.9945(6)	19.8184(9)	22.8310(10)
α	90	90	79.058(2)	65.904(19)	90	74.1510(10)	90	90	90	90
β	106.791(2)	90	66.803(2)	88.38(2)	92.1450(10)	84.7760(10)	91.0670(10)	100.1560(10)	98.9030(10)	93.562(3)
γ	90	90	72.676(2)	89.140(19)	90	68.3620(10)	90	90	90	90
Unit-cell volume *V* (Å^3)	863.62(9)	2633.7(2)	623.04(5)	993.3(4)	1134.22(5)	708.10(4)	690.07(3)	2655.54(13)	875.74(7)	1421.13(13)
ρ_{cal} (g·cm^{-3})	1.294	1.267[a]	1.323	1.392	1.258	1.343	1.378	1.310	1.359	1.362
μ (mm^{-1})	0.079	0.662	0.083	0.682	0.652	0.655	0.672	0.644	0.098	0.750
Measured/independent Reflections	21578/1983	24726/4548	20330/3670	5797/3014	13308/1812	25327/ 2392	14444/1140	85377/4357	43633/2007	23978/2274
R_{int}	0.0359	0.0317	0.0279	0.1045	0.0418	0.0476	0.0523	0.0412	0.0419	0.1375
Observed Reflections [I>2σ(I)]	1421	4454	2640	1474	1493	1958	959	3650	1674	1471
R_1[a], wR_2[b] [I>2σ(I)]	0.0483, 0.1190	0.0273, 0.0697	0.0516, 0.1305	0.1199, 0.3400	0.0529, 0.1346	0.0394, 0.0920	0.0393, 0.0947	0.0395, 0.1008	0.0695, 0.2122	0.0577, 0.1355
R_1, wR_2 (all data)	0.0728, 0.1308	0.0280, 0.0702	0.0754, 0.1404	0.2018, 0.3690	0.0645, 0.1464	0.0519, 0.1019	0.0509, 0.1066	0.0503, 0.1114	0.0814, 0.2229	0.0980, 0.1525
Goodness-of-fit on F^2	0.0971	1.063	1.046	1.096	1.079	1.081	1.049	1.109	1.100	1.028

[a]For this crystal additional water molecules are present in the structural channels. However, their positions are highly disordered and their occupancy changes due to the exchange with the atmospheric water; therefore, they were masked in the refinement and not taken into account for calculation of the molar mass of the moiety and the density of the crystal.

Table S4. Single crystal X-ray crystallographic detail of compound **sql-5-Ni-4i**.

Compound	**sql-5-Ni-4i**
Formula	$C_{52}H_{40}N_{14}NiO_6$
M(g·mol^{-1})	1015.69
T(K)	100(2)
λ(Å)	1.54178
Crystal System	Monoclinic
Space Group	$P2_1/c$
Z/Z'	4/1
Unit-cell parameters (Å/°): a b c α β γ	 10.3045(5) 15.1144(8) 30.0078(15) 90 90.994(3) 90
Unit-cell volume V (Å^3)	4673.0(4)
ρ_{cal} (g·cm^{-3})	1.444
μ (mm^{-1})	1.173
Measured/independent Reflections	62622/7902
R_{int}	0.0502
Observed Reflections [I>2σ(I)]	6588
R_1[a], wR_2[b] [I>2σ(I)]	0.0545, 0.1473
R_1, wR_2 (all data)	0.0662, 0.1549
Goodness-of-fit on F^2	1.039

X-ray Crystal Structure Description

***N,N'*-Bis(4-pyridylmethylene)naphthalene-1,5-diamine (2).** Crystal structure of **2** has been previously reported (XAPTEO).[9,10] Herein, we report a new polymorph of **2** obtained by slow evaporation of a solution of **2** in MeOH/$CHCl_3$. This polymorph crystallizes in $P2_1/n$ space group with half molecule of **2** comprising the asymmetric unit. The crystal structure was found to contain multiple symmetry equivalent weak C–H···N hydrogen bonds ($d_{C–H···N}$ = 2.821(1) Å, $D_{C···N}$ = 3.610(1) Å, $\angle_{C–H···N}$ = 143.40(1)°) between the pyridine rings of adjacent molecules that form zigzag chains (Figure 34a). Such adjacent chains in turn are associated *via* π-π stacking interactions into 3D network (Figure 34).

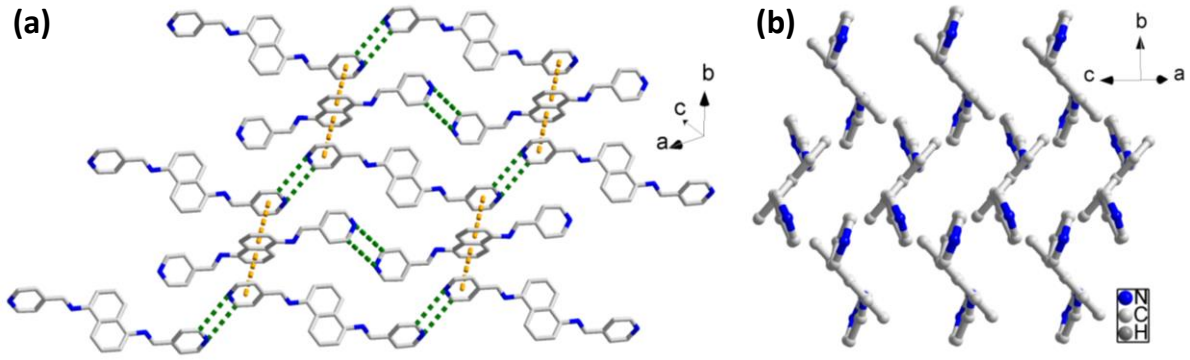

Figure S34. (a) C–H···N hydrogen bonds (green) between pyridyl rings of **2** in zigzag chains, which are in turn linked by π-π stacking interactions (yellow). (b) Crystal packing of **2**.

***N*-(pyridin-4-ylmethylene)quinolin-5-amine (3•xH_2O).** Needle-shaped crystals of **3**•xH_2O were isolated by slow evaporation of 50 mg of **3** in 4.5 mL of MeCN over a period of 4 d (88.1% yield). Compound **3**•xH_2O crystallizes in the orthorhombic space group $Pna2_1$ with two molecules of **3** and two disordered molecules of water comprising the asymmetric unit. Additional water molecules occupy the channels along *c*-axis. However, due to the rapid motion, disorder and changing occupancy, determining the exact positions and stoichiometry of water in this crystal structure was not possible. Therefore, the electron density corresponding to these molecules was masked using Olex2 software. Two crystallographically independent water molecules form chains down *c*-axis (O-H···O H-bonds; $d_{O–H···O}$ = 1.611(1) Å, $D_{O···O}$ = 2.464(1) Å, $\angle_{O–H···O}$ = 166.61(1)°; $d_{O–H···O}$ = 1.910(1) Å, $D_{O···O}$ = 2.773(1)Å, $\angle_{O–H···O}$ = 172.11(1)°;). However, due to the disorder of water molecules, those chains can be interrupted. Regardless the disorder, H_2O molecules bind to the aromatic nitrogen and carbon atoms of **3** either *via* O–H···N ($d_{O–H···N}$ = 2.010(1) Å, $D_{O···N}$ = 2.864(1) Å, $\angle_{O–H···N}$ = 166.23(1)°; $d_{C–H···N}$ = 1.939(1) Å, $D_{C···N}$ = 2.894(1) Å, $\angle_{C–H···N}$ = 155.23(1)°; $d_{O–H···N}$ = 2.025(1) Å, $D_{O···N}$ = 2.773(1) Å, $\angle_{O–H···N}$ = 135.87(1)°) or C–H···O hydrogen bonds ($d_{C–H···O}$ = 2.419(1) Å, $D_{C···O}$ = 3.240(1) Å, $\angle_{C–H···O}$ = 144.54(1)°) (Figure S35).

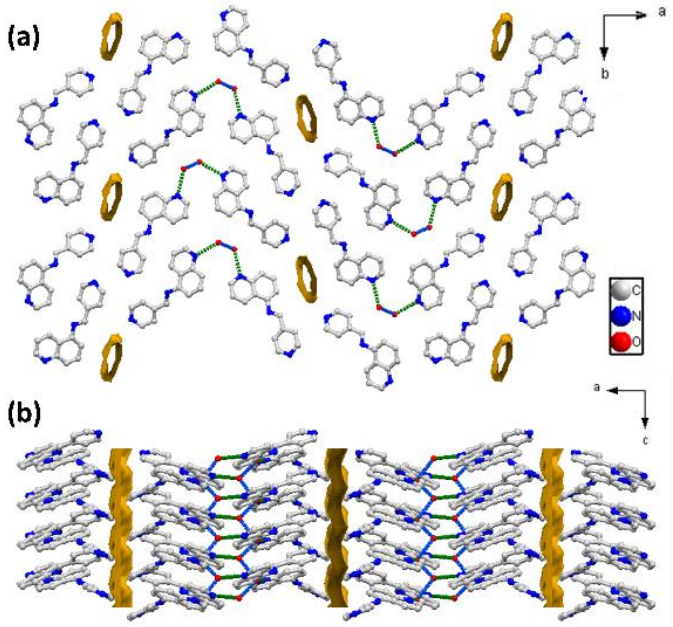

Figure S35. Crystal packing of **3**•xH_2O shown along (a) *c*- and (b) *b*-axes. Water chains down *c*-axis are marked with blue dashed lines, and solvent accessible voids are marked in yellow (Mercury software; probe radius = 1.2 Å, grid spacing = 0.7 Å).

***N,N'*-4-(1H-imidazol-1-yl)-*N*-(pyridin-4-ylmethylene)aniline (4).** Pale yellow crystals of **4** were isolated upon slow evaporation of a solution of **4** in 2.5 mL of DMF/MeOH (1:4 *v/v*) mixture over a period of 2 weeks (74.3% yield). Compound **4** crystallizes in the triclinic space group $P\bar{1}$ with one molecule of **4** comprising the asymmetric unit. Head-to-head association of molecules as a result of C–H···N H-bonding lead to formation of 1D chains (imidazoyl-imidazoyl: $d_{C–H\cdots N}$ = 2.813(1) Å, $D_{C\cdots N}$ = 3.543(1) Å, $\angle_{C–H\cdots N}$ = 136.14(1)° and pyridyl-pyridyl: $d_{C–H\cdots N}$ = 2.976(1) Å, $D_{C\cdots N}$ = 3.530(1) Å, $\angle_{C–H\cdots N}$ = 119.68(1)°). Each of these chains in turn is surrounded by six other neighboring chains (Figure S36).

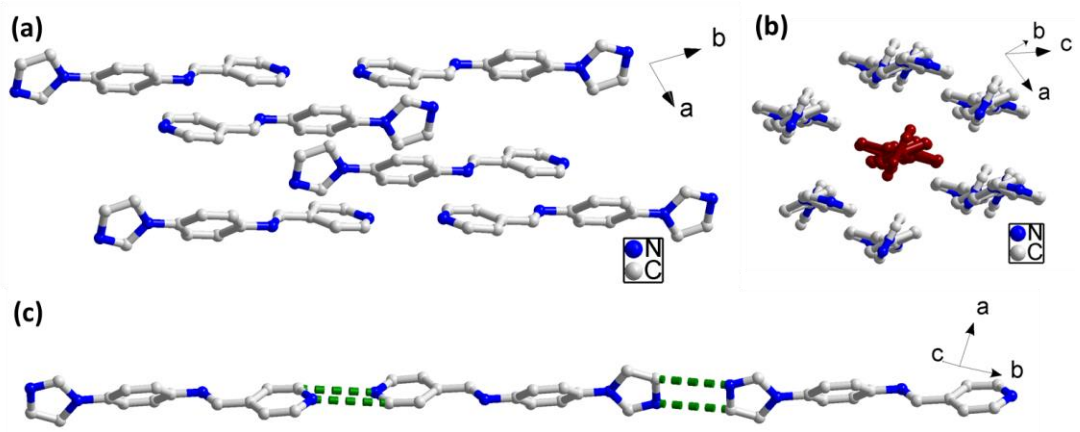

Figure S36. (a) Crystal packing of **4** down crystallographic *b*-axis. (b) Each chain is surrounded by six neighboring chains.

***N,N′*-(1,4-phenylenebis(methan-1-yl-1-ylidene))bis(4-(1H-imidazol-1-yl)aniline) (5).** Yellow needles were isolated by slow evaporation of **5** (20 mg, 0.04 mmol) in 4 mL of MeOH/$CHCl_3$ (1:1 *v/v*) mixture over a period of 6 d (97.4% yield). Compound **5** crystallizes in the triclinic space group $P\bar{1}$ with two crystallographically independent halves of the **5** molecule comprising the asymmetric unit. The imidazolyl moieties in each molecule are C-H···N H-bonded to form 1D chains ($d_{C–H···N}$ = 2.848(1) Å, $D_{C···N}$ = 3.440(1) Å, $\angle_{C–H···N}$ = 121.34(3)°), Figure 37a. Each of these 1D chains are in turn associated to six neighboring chains *via* multiple C–H···π interactions (see Table S3) as shown in Figures S37b,c.

Table S3. The dimensions of C-H···π contacts in crystal structure of **5**.

C-H···π	1	2	3	4	5
$d_{C–H···π}$ (Å)	3.037(1)	2.621(1)	3.207(1)	3.047(1)	2.846(1)
$D_{C···π}$ (Å)	3.558(1)	3.383(1)	3.682(1)	3.686(1)	3.645(1)
$\angle_{C–H···π}$ (°)	116.05(3)	137.49(3)	112.86(2)	125.97(3)	142.39(3)

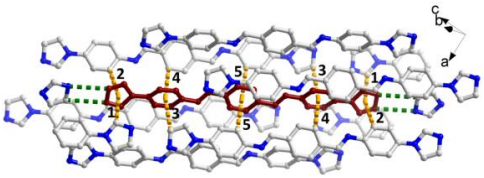

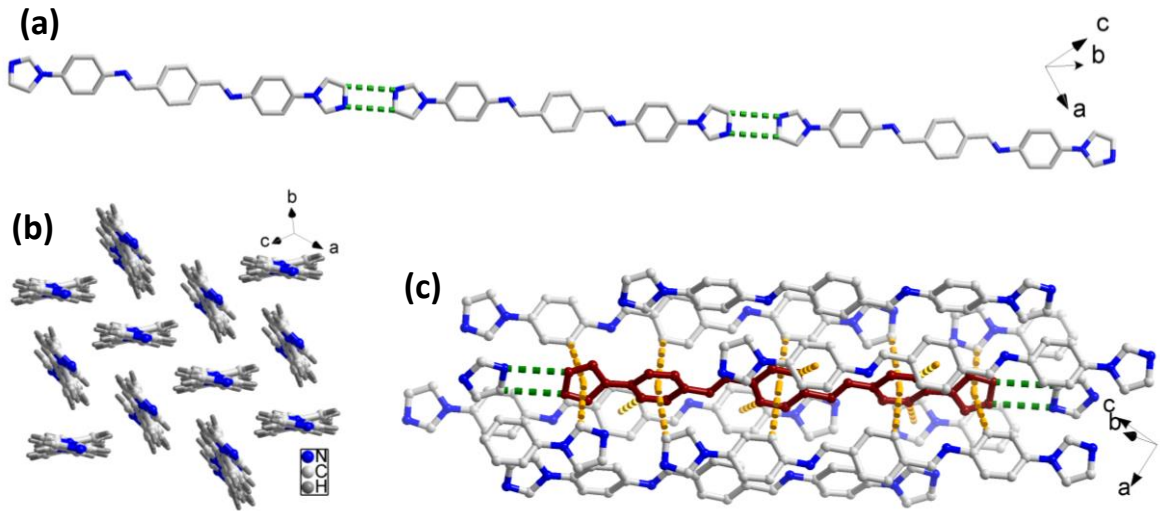

Figure S37. (a) 1D chains formed as a result of C-H···N H-bonding in compound **5**. (b) Each chain is surrounded by six neighboring chains. (c) Multiple C-H···N (green) and C-H···π (yellow) interactions around central molecule marked in red.

***N,N′*-(1,4-phenylenebis(methan-1-yl-1-ylidene))diquinolin-5-amine (6·0.6MeOH·1.4H_2O).** Deep yellow needles were isolated by slow evaporation of solution of **6** (20 mg) in 4 mL of MeOH over a period of 5 d (91.3% yield). Compound **6** crystallizes in the monoclinic space group $P2_1/c$ with half molecule of **6** and one solvent molecule (disordered between H_2O and MeOH in 7:3 ratio) comprising the asymmetric unit. Disordered H_2O and MeOH molecules occupy structural channels along *b*-axis and are connected to **6** either *via* O-H···N ($d_{O–H···N}$ = 2.046(1) Å, $D_{O···N}$ = 2.739(1) Å, $\angle_{O–H···N}$ = 135.79(1)°); $d_{O–H···N}$ = 2.094(1) Å, $D_{O···N}$ = 2.919(1) Å, $\angle_{O–H···N}$ = 157.00(1)°), C-H···O ($d_{C–H···O}$ = 2.652(1) Å, $D_{C···O}$ = 3.595(1) Å, $\angle_{C–H···O}$ = 17.95(1)°; $d_{C–H···O}$ = 2.950(1) Å, $D_{C···O}$ = 3.554(1) Å, $\angle_{C–H···O}$ = 122.74(1)°; $d_{C–H···O}$ = 2.572(1) Å, $D_{C···O}$ = 3.458(1) Å, $\angle_{C–H···O}$ = 155.29(1)°) or C-H···N H-bonds ($d_{C–H···N}$ = 2.793(1) Å, $D_{C···N}$ = 3.735(1) Å, $\angle_{C–H···N}$ = 162.37(1)°), Figure S38.

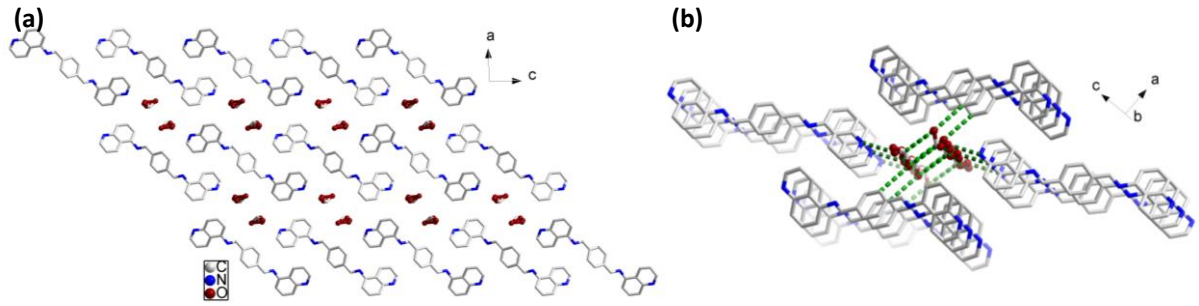

Figure S38. (a) Crystal packing of **6** down crystallographic *b*-axis. (b) H-bonding between 1D MeOH chains and the neighbouring molecules **6**.

N′,N′*-(1,4-phenylenebis(methan-1-yl-1-ylidene))dipyridin-4-amine (7)**. Compound **7** crystallizes in four different forms, two polymorphs (herein named **7*α and **7*β***), cocrystal with 4-aminopyridine (**7•AMP**) and hydrate (**7**•4H_2O). Mixture of crystals of **7*α*** and **7•AMP** were obtained after heating ground mixture of starting materials at 120°C, while recrystallization of the heated sample from various solvents (including acetone, acetonitrile and ethanol) leaded to forms **7*α***, **7*β*** and **7**•4H_2O. The hydrate of **7** transforms to anyhydrous polymorph **7*α*** after heating at 120°C. Polymorph **7*α*** is of triclinic symmetry, space group $P\bar{1}$, with two crystallographically independent halves of the **7** molecule comprising the asymmetric unit. Molecules of **7** bind to each other *via* CH···N H-bonds ($d_{C–H···N}$ = 2.712(1) Å, $D_{C···N}$ = 3.491(1) Å, $\angle_{C–H···N}$ = 139.63(1)°; $d_{C–H···N}$ = 2.701(1) Å, $D_{C···N}$ = 3.494(1) Å, $\angle_{C–H···N}$ = 141.45(1)°; $d_{C–H···N}$ = 2.749(1) Å, $D_{C···N}$ = 3.463(1) Å, $\angle_{C–H···N}$ = 132.65(2)°; $d_{C–H···N}$ = 2.651(1) Å, $D_{C···N}$ = 3.588(1) Å, $\angle_{C–H···N}$ = 168.95(1)°) creating 3D network, Figure S39(a,b), as well as π-π ($D_{π···π}$ = 3.704(1) Å; $D_{π···π}$ = 3.675(1) Å) and CH···π ($d_{C–H···π}$ = 3.127(1) Å, $D_{C···π}$ = 4.025(1) Å, $\angle_{C–H···π}$ = 158.46(1)°; $d_{C–H···π}$ = 2.735(1) Å, $D_{C···π}$ = 3.637(1) Å, $\angle_{C–H···π}$ = 158.80(1)°; $d_{C–H···π}$ = 2.744(1) Å, $D_{C···π}$ = 3.557(1) Å, $\angle_{C–H···π}$ = 144.12(1)°; $d_{C–H···π}$ = 3.292(1) Å, $D_{C···π}$ = 4.177(1) Å, $\angle_{C–H···π}$ = 155.87(1)°) interactions, Figure S39c. In polymorph **7*β***, of monoclinic space group $P2_1/c$, one crystallographically independent half of molecule of **7** comprises the asymmetric unit. Molecules of **7** bind to each other *via* CH···N hydrogen bonds ($d_{C–H···N}$ = 2.617(1) Å, $D_{C···N}$ = 3.566(1) Å, $\angle_{C–H···N}$ = 176.88(1)°), Figure S40a creating 2D sheets, stacked in direction [204] *via* π-π interactions ($d_{π-π}$ = 3.834(1) Å), Figure S40b. **7•AMP** crystallizes in $P2_1/c$ space group, with 1.5 molecules of **7** and one molecule of 4-aminopyridine comprising the asymmetric unit. Molecules of **7** interact with each other *via* CH···N hydrogen bonds ($d_{C–H···N}$ = 2.673(1) Å, $D_{C···N}$ = 3.595(1) Å, $\angle_{C–H···N}$ = 163.95(1)°; $d_{C–H···N}$ = 2.570(1) Å, $D_{C···N}$ = 3.493(1) Å, $\angle_{C–H···N}$ = 164.13(1)°; $d_{C–H···N}$ = 2.658(1) Å, $D_{C···N}$ = 3.552(1) Å, $\angle_{C–H···N}$ = 157.04(1)°) and *via* π-π interactions ($D_{π-π}$ = 3.912(1) Å, $D_{π-π}$ = 3.903(1) Å, $D_{π-π}$ = 3.974(1) Å). They are also indirectly bridged *via* chains of 4-aminopyridine molecules to which they bind with NH···N ($d_{N–H···N}$ = 2.104(1) Å, $D_{N···N}$ = 3.020(1) Å, $\angle_{N–H···N}$ = 171.63(1)°) and CH···N ($d_{C–H···N}$ = 2.641(1) Å, $D_{C···N}$ = 3.383(1) Å, $\angle_{C–H···N}$ = 135.29(1)°) hydrogen bonds. 4-Aminopyridine molecules bind to each other *via* NH···N contacts ($d_{N–H···N}$ = 2.012(1) Å, $D_{N···N}$ = 2.960(1) Å, $\angle_{N–H···N}$ = 172.83(1)°), Figure S41.

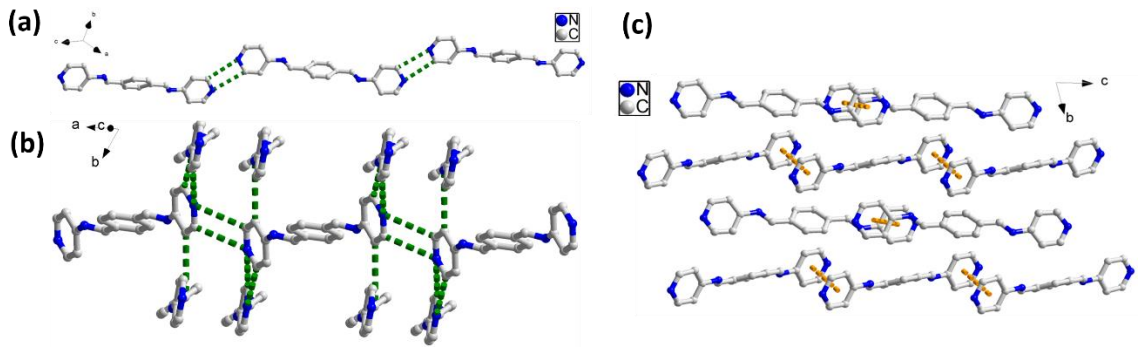

Figure S39. (a,b) C-H···N H-bonding in compound **7*α***. (c) Crystal packing of **7*α*** along *a*-axis as well as π-π stacking interactions (yellow) between pyridine moieties in compound **7*α***.

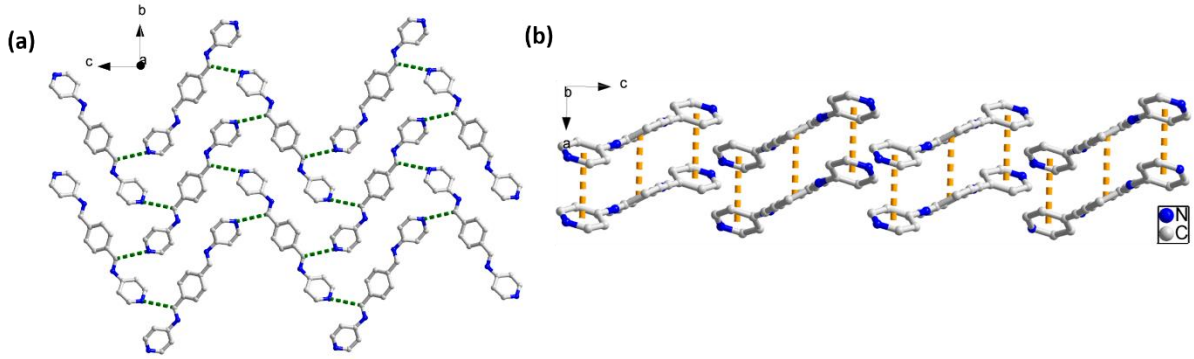

Figure S40. (a) 2D sheet formed as a result of C-H···N H-bonding in compound **7*β***. (b) Crystal packing of **7*β*** shown along *b*-axis with π-π stacking interactions between pyridine moieties in compound **7*β*** marked in yellow.

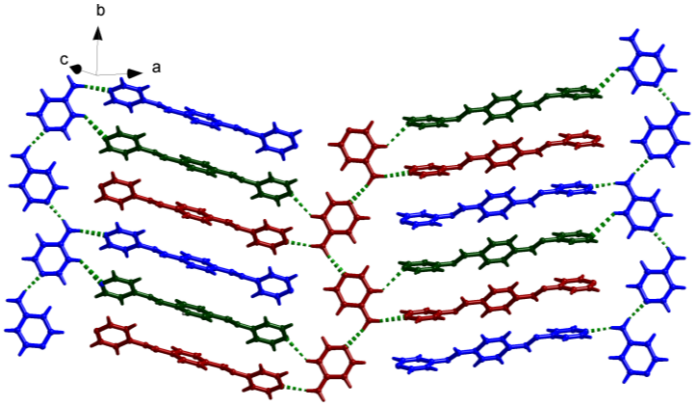

Figure S41. Chains of 4-aminopyridine molecules binding to each other *via* N-H···N H-bonding zipping the molecules of **7** *via* N-H···N H-bonds.

The hydrate of 7 (**7**•4H_2O) crystallizes in the monoclinic space group $P2_1/c$ with half molecule of **7** and two H_2O molecules comprising the asymmetric unit. Disordered water molecules occupy channels between molecules of **7** and interact with each other *via* OH···O hydrogen bonds ($d_{O–H···O}$ = 1.978(1) Å, $D_{O···O}$ = 2.760(1) Å, $\angle_{O–H···O}$ = 179.08(1)°; $d_{O–H···O}$ = 1.789(1) Å, $D_{O···O}$ = 2.315(1) Å, $\angle_{O–H···O}$ = 116.77(1)°; $d_{O–H···O}$ = 2.022(1) Å, $D_{O···O}$ = 2.831(1) Å, $\angle_{O–H···O}$ = 154.18(1)°; $d_{O–H···O}$ = 2.337(1) Å, $D_{O···O}$ = 3.156(1) Å, $\angle_{O–H···O}$ = 156.87(1)°) and with molecules of **7** *via* OH···N ($d_{O–H···N}$ = 2.016(1) Å, $D_{O···N}$ = 2.865(1) Å, $\angle_{O–H···N}$ = 164.85(1)°; $d_{O–H···N}$ = 1.930(1) Å, $D_{O···N}$ = 2.782(1) Å, $\angle_{O–H···N}$ = 165.45(1)°) and CH···O ($d_{C–H···O}$ = 2.694(1) Å, $D_{C···O}$ = 3.548(1) Å, $\angle_{C–H···O}$ = 149.94(1)°; $d_{C–H···O}$ = 2.581(1) Å, $D_{C···O}$ = 3.463(1) Å, $\angle_{C–$

$_{H\cdots O}$ = 154.59(1)°) contacts, Figure S42a. Additionally, molecules of **7** are joined with each other *via* CH···N ($d_{C–H\cdots N}$ = 2.690(1) Å, $D_{C\cdots N}$ = 3.617(1) Å, $\angle_{C–H\cdots N}$ = 165.54(1)°) contacts (Figure S42a) and via π···π interactions ($D_{\pi\cdots\pi}$ = 3.736(1) Å), Figure S42b.

In the crystal structure of hydrate of **7** (**7**•4H_2O), one of the two water molecules in the asymmetric part of the unit cell is more loosely H-bonded than the other. As a result this molecule can exhibit a movement (can be present in the multiple positions in the crystal structure). This in turn affects collected X-ray diffraction data. The possibility of many positions taken by the water molecule resulted in hard to model disorder and therefore its position was assigned at the maximum of the electron density found in corresponding region of the electron density map. However, since this position is not always occupied by water throughout the crystal, its refinement was affected and resulted in negative residual density nearby assigned position of atom O_2 of the water molecule. The presence of 2 water molecules in the asymmetric part of the unit cell (4 water molecules per one molecule of the organic compound) was confirmed with TGA.

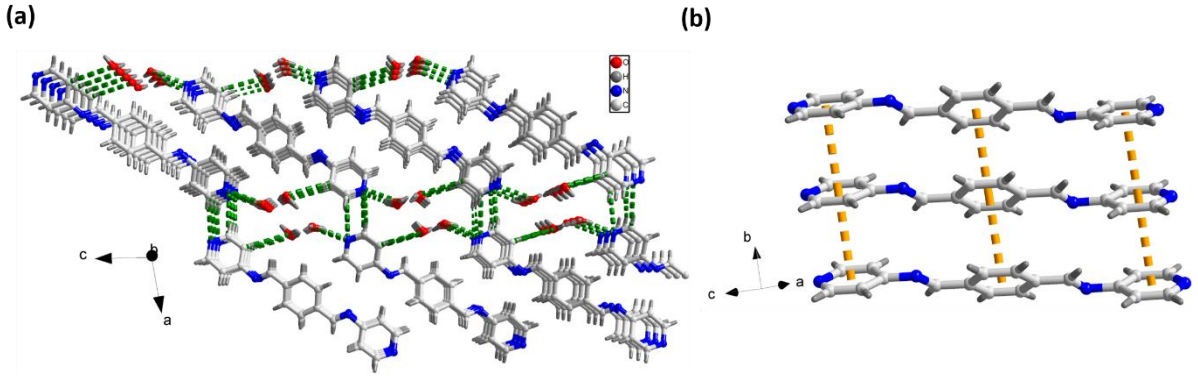

Figure S42. (a) Crystal packing of **7**•4H_2O along *b*-axis showing NH···N, OH···N and CH···O H-bonds. (b) π-π stacking interactions (yellow) between molecules of **7**•4H_2O.

4-((4-(1H-imidazol-1-yl)phenylimino)methyl)benzoic acid (8). Pale yellow plates were obtained by slow evaporation of **8** (30 mg, 0.1 mmol) in 8 mL of MeOH/$CHCl_3$ (1:1 *v/v*) mixture over a period of 5 d (93.5% yield). Compound **8** crystallizes in the monoclinic space group $P2_1/c$ with one **8** molecule comprising the asymmetric unit. Crystal packing analysis reveals the presence of imidazolyl-carboxyl *supramolecular heterosynthon*[11,12] (O–H···N H-bonds: $d_{O–H\cdots N}$ = 1.836(1) Å, $D_{O\cdots N}$ = 2.652(1) Å, $\angle_{O–H\cdots N}$ = 173.80(1)°) leading to formation of 1D zigzag chains that aggregate in (104) plane, Figure S43a. The 2D sheets thus formed are in turn found to stack along in [104] direction (Figure S43b) *via* C–H···N H-bonds between phenyl moiety in **8** belonging to one sheet and the imine moiety of **8** belonging to the neighboring sheet ($d_{C–H\cdots N}$ = 3.019(1) Å, $D_{C\cdots N}$ = 3.937(1) Å, $\angle_{C–H\cdots N}$ = 169.17(1)°), as well as C–H···O H-bonds between phenyl moiety and carboxyl group of adjacent sheets ($d_{C–H\cdots O}$ = 2.558(1) Å, $D_{C\cdots O}$ = 3.475(1) Å, $\angle_{C–H\cdots O}$ = 168.82(1)°).

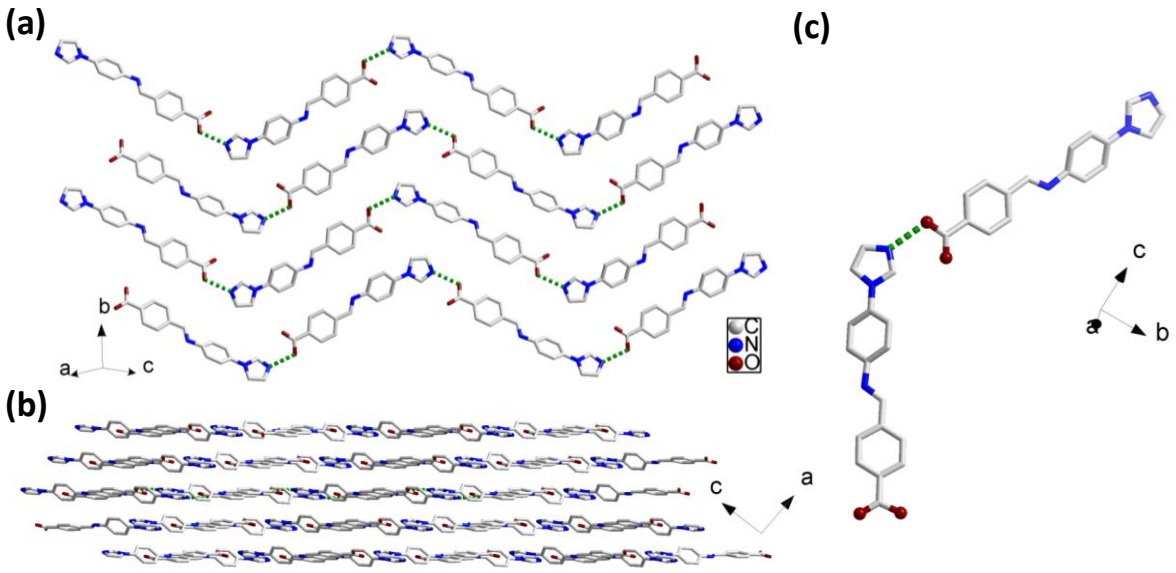

Figure S43. (a) 1D zigzag chains that aggregate to form 2D sheets for compound **8**. (b) 2D sheets stacked along direction [104]. (c) Imidazoyl-carboxyl supramolecular heterosynthon.

REFERENCES

1. G. M. Sheldrick, (2008). *SADABS. Program for Empirical Absorption Correction*. University of Gottingen, Germany.
2. O. V. Dolomanov, L. J. Bourhis, R. J. Gildea, J. A. K. Howard and H. Puschmann, *J. Appl. Cryst.*, 2009, **42**, 339-341.
3. G. M. Sheldrick, *Acta Cryst. A*, 2008, **A64**, 112-122.
4. G. M. Sheldrick, *Acta Cryst. A*, 2015, **71**, 3-8.
5. G. M. Sheldrick, *Acta Cryst. C*, 2015, **71**, 3-8.
6. D. Sek, M. Siwy, K. Bijak, M. Grucela-Zajac, G. Malecki, K. Smolarek, L. Bujak, S. Mackowski and E. Schab-Balcerzak, *J. Phys. Chem. A*, 2013, **117**, 10320-10332.
7. V. Safarifard, S. Rodríguez-Hermida, V. Guillerm, I. Imaz, M. Bigdeli, A. Azhdari Tehrani, J. Juanhuix, A. Morsali, M. E. Casco, J. Silvestre-Albero, E. V. Ramos-Fernandez and D. Maspoch, *Cryst. Growth Des.*, 2016, **16**, 6016-6023.
8. J. Nandi and V. K. Sankar, *J. Pharm. Sci. Innov.*, 2012, **1**, 9-11.
9. Y.-R. Liu, X.-P. Li, J.-A. Zhang and C.-Y. Su, *Acta Cryst. E*, 2005, **61**, o2089-o2090.
10. D. W. Min, B. Y. Cho and S. W. Lee, *Inorg. Chim. Acta*, 2006, **359**, 577-584.
11. H. D. Clarke, K. K. Arora, Bass, H.; Kavuru, P.; Ong, T. T.; Pujari, T.; Wojtas, L.; Zaworotko, M. J. *Cryst. Growth Des.*, 2010, **10**, 2152-2167.
12. R. D. B. Walsh, M. W. Bradner, S. Fleischman, L. A. Morales, B. Moulton, N. Rodriguez-Hornedo and M. J. Zaworotko, *Chem. Commun.*, 2003, **0**, 186-187.